N21/5:6/2348
GOVT. DOC.
NACA TN 2348

NATIONAL ADVISORY COMMITTEE FOR AERONAUTICS

TECHNICAL NOTE 2348

EFFECT OF ASPECT RATIO ON THE LOW-SPEED LATERAL CONTROL CHARACTERISTICS OF UNSWEPT UNTAPERED LOW-ASPECT-RATIO WINGS

By Rodger L. Naeseth and William M. O'Hare

Langley Aeronautical Laboratory
Langley Field, Va.

Washington
May 1951

CONN. STATE LIBRARY
BUSINESS, SCIENCE & TECHNOLOGY DEP'T.
MAY 10 1951

NATIONAL ADVISORY COMMITTEE FOR AERONAUTICS

TECHNICAL NOTE 2348

EFFECT OF ASPECT RATIO ON THE LOW-SPEED LATERAL CONTROL CHARACTERISTICS OF UNSWEPT UNTAPERED LOW-ASPECT-RATIO WINGS

By Rodger L. Naeseth and William M. O'Hare

SUMMARY

A low-speed investigation was made to determine the lateral control characteristics for a series of unswept, untapered, complete wings of aspect ratios 1.13, 2.13, 4.13, and 6.13. The wings were equipped with 0.25-chord sealed ailerons of various spans and of various spanwise locations.

The variation of experimental aileron effectiveness with wing aspect ratio was not accurately predicted for all spans of aileron by any one of the three theoretical methods with which a comparison was made.

Design charts based on the experimental results are presented for estimating the aileron effectiveness for low-aspect-ratio, untapered, unswept wings.

INTRODUCTION

Increased interest in the use of low-aspect-ratio wings for high-speed aircraft and missiles, because their use would delay the onset of or reduce adverse compressibility effects (reference 1), has resulted in a need for the determination of their aerodynamic characteristics throughout the speed range. Results of several investigations to determine the longitudinal characteristics of low-aspect-ratio wings are available, but little work has been done to determine the lateral control characteristics of wings of aspect ratios less than 6.

Accordingly, a series of unswept, untapered, complete wings of aspect ratios 1.13, 2.13, 4.13, and 6.13 was investigated at a Mach number of 0.26 to determine the effect of aspect ratio on the lateral control characteristics of the wings equipped with 0.25-chord plain ailerons of various spans and of various spanwise locations.

The lateral control characteristics as well as basic aerodynamic characteristics and lateral-stability parameters of the wings are presented herein. Estimates of aileron effectiveness made by means of several theories are compared herein with the experimental results.

COEFFICIENTS AND SYMBOLS

The data are referred to the stability axes (fig. 1), which are a system of axes with the origin at the center of moments (0.25 M.A.C. (fig. 2)). The Z-axis is in the plane of symmetry and perpendicular to the relative wind, the X-axis is in the plane of symmetry and perpendicular to the Z-axis, and the Y-axis is perpendicular to the plane of symmetry.

The coefficients and symbols used are defined as follows:

C_L	lift coefficient (Lift/qS)
C_D	drag coefficient (Drag/qS)
C_Y	lateral-force coefficient (Y/qS)
C_m	pitching-moment coefficient ($M/qS\bar{c}$)
C_l	rolling-moment coefficient (L/qSb)
C_n	yawing-moment coefficient (N/qSb)
Y	lateral force, pounds
M	pitching moment about Y-axis, foot-pounds
L	rolling moment about X-axis, foot-pounds
N	yawing moment about Z-axis, foot-pounds
S	wing area, square feet
q	free-stream dynamic pressure, pounds per square foot $\left(\frac{1}{2}\rho V^2\right)$
A	aspect ratio (b^2/S)
V	free-stream velocity, feet per second
ρ	mass density of air, slugs per cubic foot

c local wing chord, feet

$\bar{c}$ wing mean aerodynamic chord, feet $\left(\frac{2}{S}\int_0^{b/2} c^2 dy\right)$

c_a local aileron chord, feet

b wing span, feet

b_a aileron span, feet

y lateral distance from plane of symmetry, measured parallel to Y-axis, feet

y_o lateral distance from plane of symmetry to outboard end of aileron, measured parallel to Y-axis, feet

y_i lateral distance from plane of symmetry to inboard end of aileron, measured parallel to Y-axis, feet

α angle of attack of wing-chord plane, degrees

ψ angle of yaw (angle between relative wind and plane of symmetry), measured in XY-plane, degrees

δ_a aileron deflection relative to wing-chord plane, measured in a plane perpendicular to aileron hinge axis and positive when trailing edge is down, degrees

$Cl/\Delta\alpha$ rolling-moment coefficient produced by 1° difference in angle of attack of various right and left parts of a complete wing

α_δ flap-effectiveness parameter, that is, effective change in wing angle of attack caused by unit angular change in control-surface deflection

$\left(\frac{L}{D}\right)_{max}$ maximum ratio of lift to drag

$C_{L_\alpha} = \left(\frac{\partial C_L}{\partial \alpha}\right)_{\delta_a=0^\circ}$ measured near $\alpha = 0^\circ$

$C_{l_{\delta_a}'} = \left(\frac{\partial C_l}{\partial \delta_a}\right)_{\alpha=0^\circ}$ measured near $\delta_a = 0^\circ$

$C_{l_\psi} = \frac{\partial C_l}{\partial \psi}$

$C_{n_\psi} = \frac{\partial C_n}{\partial \psi}$

$C_{Y_\psi} = \frac{\partial C_Y}{\partial \psi}$

Subscripts:

max maximum

A any aspect ratio unless value of A is given as in $\left(\frac{C_l}{\Delta\alpha}\right)_{A=6}$

Rolling-moment and yawing-moment coefficients represent the aerodynamic moments on a complete wing produced by deflection of the aileron on only the right semispan of the wing.

MODEL AND APPARATUS

Each complete-wing model was mounted horizontally on a single strut support in the Langley 300 MPH 7- by 10-foot tunnel, and all forces and moments acting on the model were measured by means of the tunnel balance system.

The geometric characteristics of the untapered, unswept, complete-wing models investigated are itemized in table I and sketches of the models are given in figure 2. The wing models had NACA 64A010 airfoil sections, and the wing tips were formed by rotating the airfoil sections to produce bodies of revolution. The models were constructed of a laminated mahogany and steel core enclosed in a covering composed of $\frac{1}{32}$-inch sheet aluminum glued between sheets of $\frac{1}{32}$-inch fir. The right semispan of each wing was equipped with a 0.25c aluminum flap divided into four parts. The deflection of each flap segment was adjusted by means of hinge clamps. The hinge-line gap and all chordwise gaps between flap segments of equal deflection were sealed for

all tests. Because the wings of aspect ratio 6.13 and 4.13 were thin, bodies of revolution (fig. 2) were used as fairings to enclose the strut pivot and thereby permit more accurate determination of strut tare effects.

TESTS

All the tests were performed in the Langley 300 MPH 7- by 10-foot tunnel at an average dynamic pressure of approximately 99 pounds per square foot, which corresponds to a Mach number of 0.26. Reynolds numbers, based on each wing mean aerodynamic chord, were as follows:

Wing aspect ratio	Reynolds number
6.13	1,800,000
4.13	2,200,000
2.13	3,100,000
1.13	4,300,000

Data for each test were obtained through an angle-of-attack range from -6° to beyond the wing stall. Lift, drag, and pitching-moment data were obtained for each wing at $\psi = 0^\circ$ with $\delta_a = 0^\circ$, and tests were made at $\psi = \pm 5^\circ$ to obtain the lateral-stability derivatives of each model at $\delta_a = 0^\circ$. Lateral-control data were obtained for each of the wings with the various spans of inboard and outboard ailerons listed in table II through a deflection range of $\pm 20^\circ$, except for the $A = 1.13$ wing model for which the deflection range extended to $\pm 30^\circ$.

CORRECTIONS

Jet-boundary (induced upwash) corrections were applied to the angle of attack and the drag and rolling-moment coefficients according to the methods of reference 2. The data were also corrected for blockage effects by the method of reference 3 and for model-support-strut tares.

PRESENTATION OF EXPERIMENTAL DATA

Lift, drag, and pitching-moment characteristics of the four wing models are presented in figure 3. The variation of C_{L_α}, $C_{L_{max}}$,

$(L/D)_{max}$, and aerodynamic-center location with wing aspect ratio is shown in figure 4. The variation of the lateral-stability derivatives C_{l_ψ}, C_{n_ψ}, and C_{Y_ψ} with lift coefficient obtained for each model is given in figure 5.

Rolling-moment-coefficient and yawing-moment-coefficient data obtained through the angle-of-attack range for each of the four wings equipped with various spans of outboard and inboard ailerons are presented in figures 6 to 29. Cross plots of C_l against δ_a at $\alpha \approx 0^\circ$ for the aileron spans tested on the four wings are given in figure 30. The slopes of the curves of C_l against δ_a for outboard ailerons, measured at $\delta_a = 0^\circ$ in figure 30, are presented in figure 31 as a function of $\frac{y_i}{b/2}$.

DISCUSSION

Wing Aerodynamic Characteristics

The data of figure 3 show fairly regular variations of α, C_D, and C_m with C_L except for the $A = 1.13$ wing. The lift curve of the $A = 1.13$ wing exhibited a break between $\alpha = 16^\circ$ and 18°, and a corresponding rapid drag rise and a large change in pitching-moment coefficient toward more negative values occurred in this α range. Observation of the tufts on this wing showed that this phenomenon occurred as a result of a sudden leading-edge separation which left only the tufts in the region of the wing tips definitely steady. With decrease in the angle of attack, observation of the tufts indicated that the flow reattached at about the same value of α and over an equally small increment of α. This phenomenon may be a function of the Reynolds number of the tests and may not exist at flight Reynolds numbers.

The wing lift-curve slopes increased with increasing aspect ratio (fig. 4) and the variation of C_{L_α} with aspect ratio was accurately predicted by the method of reference 4. The variation of maximum lift coefficient and $(L/D)_{max}$ with aspect ratio is similar to that reported in reference 5 in which an investigation of low-aspect-ratio wings of Clark Y airfoil section indicated a peak value of the maximum lift coefficient at about $A = 1$ and an increase in $(L/D)_{max}$ with increasing aspect ratio. The aerodynamic center of each wing model, measured at low lift coefficients, was ahead of its respective quarter chord of the mean aerodynamic chord. This distance was small for the $A = 2.13$, 4.13,

and 6.13 wing models but became significant for the $A = 1.13$ wing model. As indicated in figure 3, above $C_L \approx 0.5$ all of the pitching-moment curves became stable.

Lateral Stability Characteristics

The effective dihedral parameter C_{l_ψ} increased approximately linearly with increasing C_L until the wing began to stall (fig. 5). Since the extent of the lift-coefficient range wherein C_{l_ψ} varies linearly with C_L is a function of Reynolds number (unpublished data), the experimental data are not necessarily indicative of the variation of C_{l_ψ} with C_L near the wing stall for flight Reynolds number. The slopes of the curves of C_{l_ψ} plotted against C_L measured near $C_L = 0$ increased with decreasing aspect ratio; this variation of C_{l_ψ} with C_L for various aspect ratios agrees qualitatively with the variation reported in reference 6.

Throughout the lift-coefficient range, the values of C_{n_ψ} and C_{Y_ψ} were small. The values of C_{n_ψ} were generally slightly negative and these negative values indicate positive directional stability.

Lateral Control Characteristics

Rolling-moment characteristics.- The data for the $A = 1.13$ wing (figs. 6 to 11) indicate a rapid loss in aileron effectiveness at an angle of attack considerably below the plain-wing stall but approximately the same as or slightly above that angle at which the leading-edge separation previously described occurred. Below this angle the curves of rolling moment against angle of attack indicate fairly constant rolling moments for all deflections.

The curves of rolling moment against angle of attack for the $A = 2.13$ wing (figs. 12 to 17) show relatively constant rolling moments over the angle-of-attack range up to the angle of attack for plain-wing stall.

The data for the $A = 4.13$ and 6.13 wings (figs. 18 to 29) indicate generally constant rolling moments up to the angle of attack for plain-wing stall for negative aileron deflections. The rolling moments

produced by positive deflections, however, tended to approach zero at a lower angle of attack as the aileron deflection was increased. This effect was more pronounced for the larger-span ailerons.

In general, the $A = 1.13$ wing gave fairly constant rolling moments over an increased angle-of-attack range for greater aileron deflections than did the higher-aspect-ratio wings.

The curve of C_l plotted against δ_a at $\alpha \approx 0^\circ$ for the $A = 6.13$ wing shows a decrease in effectiveness at about $\delta_a = 15^\circ$; whereas the curves of C_l plotted against δ_a for the wings of lower aspect ratio have generally constant slopes through the deflection ranges tested (for $A = 4.13$ and 2.13, $\delta_a = \pm 20^\circ$; for $A = 1.13$, $\delta_a = \pm 30^\circ$) (fig. 30).

The spanwise-effectiveness curves of the ailerons on the four wings (fig. 31) show that aileron effectiveness decreases as aileron span or wing aspect ratio decreases. However, because the damping in roll also decreases with decreasing aspect ratio (reference 7), the ratio of control-surface area to wing area required to maintain a constant rolling effectiveness will not show so great a variation with decreasing aspect ratio as indicated by the aileron-effectiveness data. The rolling-moment data of figures 30 and 31 show that spanwise-effectiveness curves based on the effectiveness of outboard ailerons can be used to estimate the effectiveness of inboard ailerons (reference 8) because the value of $C_{l_{\delta_a}}$ for an aileron spanning any portion of the wing is the difference between the values of $C_{l_{\delta_a}}$ at the inboard end and $C_{l_{\delta_a}}$ at the outboard end of the aileron. The effectiveness of the inboard ailerons estimated in this manner agrees reasonably well with the corresponding values of $C_{l_{\delta_a}}$ determined from figure 30. A comparison of the values of $C_{l_{\delta_a}}$ for inboard and outboard ailerons (fig. 30 or 31) shows that outboard ailerons are more effective than inboard ailerons of the same span.

A comparison of the aileron effectiveness computed by three existing methods (references 9 to 11) and the experimental values of $C_{l_{\delta_a}}$ are presented in figure 32 for outboard-control spans of $\frac{b_a}{b/2} = 1.00$, 0.60, and 0.30. The results presented in reference 9 include the data of reference 8, extrapolated for aspect ratios between 4 and 2. The method of reference 10 is an application of the Weissinger method. A value of α_δ of 0.54 was used in the theoretical computations. This

value was based on NACA 64A010 section data for $\frac{c_a}{c} = 0.30$ (reference 12) corrected to $\frac{c_a}{c} = 0.25$ by the trends given in reference 9. Throughout the aspect-ratio range of 2 to 6, values of $C_{l_{\delta_a}}$ computed by the method of reference 9 were in better quantitative agreement with the experimental results than the values of $C_{l_{\delta_a}}$ computed by the method of reference 10; however, the trend of the experimental data was more accurately predicted by reference 10 than by reference 9. For a wing of $A = 6$ with controls of about 30 percent span, it was noted that the experimental values of $C_{l_{\delta_a}}$ agreed well with the values estimated by the method of reference 9. The agreement would be similar for an $A = 6$ wing with controls of smaller span. However, values of $C_{l_{\delta_a}}$ computed by the method of reference 9 are considerably lower than the large experimental values of $C_{l_{\delta_a}}$ produced by full-span ailerons on the $A = 6$ wing. In an effort to resolve this discrepancy, a survey was made of experimental aileron-effectiveness data for $A = 6$ wings equipped with various flap ailerons. The experimental values of aileron effectiveness for these $A = 6$ wings were compared with values computed by the method of reference 9. Most of the aileron configurations yielded values of $C_{l_{\delta_a}}$ of 0.0020 or less, which agreed fairly well with computed values. The meager data available for aileron configurations which gave values of $C_{l_{\delta_a}}$ much greater than 0.0020 indicated that these large values of $C_{l_{\delta_a}}$ were consistently higher than computed values for these configurations.

The method of reference 11, which predicts a linear variation of $C_{l_{\delta_a}}$ with aspect ratio (fig. 32), is based on lifting-line theory of zero-aspect-ratio wings at low speeds or wings of moderate aspect ratio at the speed of sound. The theory states that $C_{l_{\delta_a}}$ is independent of the chordwise position of the control hinge line, or effectively, $\alpha_\delta = 1$. The low-speed application of this method appears to be limited to wings of aspect ratios less than 1.

Because the theoretical methods were not entirely satisfactory, the experimental data were reduced to a convenient form (figs. 33 and 34) for predicting aileron effectiveness of low-aspect-ratio, unswept, untapered wings. The method used is similar to that of reference 9. The aileron-effectiveness data of figure 31 were reduced to values of $C_l/\Delta\alpha$ for $A = 6$ and to the aspect-ratio factor K which is the ratio of $C_l/\Delta\alpha$ for any A to $C_l/\Delta\alpha$ for $A = 6$. These values and the equation

relating them are given in figures 33 and 34. The factor K showed only a slight and inconsistent variation with $\frac{y_i}{b/2}$ and therefore was assumed to be independent of aileron span in these computations. By use of the curves of figures 33 and 34 and appropriate values of α_δ (such as are presented in reference 9), the effectiveness of ailerons on low-aspect-ratio, unswept, untapered wings may be estimated.

Yawing-moment characteristics.- The total yawing-moment coefficient resulting from equal up-and-down deflections of the ailerons was approximately zero at small angles of attack but became adverse (sign of yawing moment opposite to sign of rolling moment) as α was increased and as the aileron deflection was increased.

The negative values of the C_n/C_l ratio for each wing did not exceed -0.2 for lift coefficients equal to or less than $0.9C_{L_{max}}$, except for the $A = 1.13$ wing for which a sharp rise in $-C_n/C_l$ is judged to reflect the abnormally high values of drag above $C_L \approx 0.55$ previously discussed. For the range of aspect ratio investigated, it appears that the problems associated with adverse yawing moments on unswept wings of moderate aspect ratio become serious well below $C_{L_{max}}$ if partial flow separation in the linear lift range is characteristic of the wings.

CONCLUSIONS

The results of a low-speed investigation made to determine the lateral control characteristics for a series of unswept, untapered wings of aspect ratio 1.13, 2.13, 4.13, and 6.13 equipped with 0.25-chord sealed ailerons of various spans and of various spanwise locations indicated the following conclusions:

1. The variation of experimental aileron effectiveness with aspect ratio was not accurately predicted for all spans of ailerons by any one of the three theoretical methods with which a comparison was made.

2. The problems associated with adverse yawing moments become serious well below maximum lift coefficient for unswept wings of moderately low aspect ratio if partial flow separation in the linear lift range is characteristic of the wings.

3. Aileron effectiveness decreased as aileron span or wing aspect ratio was decreased.

Langley Aeronautical Laboratory
National Advisory Committee for Aeronautics
Langley Field, Va., February 1, 1951

REFERENCES

1. Stack, John, and Lindsey, W. F.: Characteristics of Low-Aspect-Ratio Wings at Supercritical Mach Numbers. NACA Rep. 922, 1949.

2. Gillis, Clarence L., Polhamus, Edward C., and Gray, Joseph L., Jr.: Charts for Determining Jet-Boundary Corrections for Complete Models in 7- by 10-Foot Closed Rectangular Wind Tunnels. NACA ARR L5G31, 1945.

3. Herriot, John G.: Blockage Corrections for Three-Dimensional-Flow Closed-Throat Wind Tunnels, with Consideration of the Effect of Compressibility. NACA Rep. 995, 1950.

4. Polhamus, Edward C.: A Simple Method of Estimating the Subsonic Lift and Damping in Roll of Sweptback Wings. NACA TN 1862, 1949.

5. Zimmerman, C. H.: Characteristics of Clark Y Airfoils of Small Aspect Ratios. NACA Rep. 431, 1932.

6. Goodman, Alex, and Brewer, Jack D.: Investigation at Low Speeds of the Effect of Aspect Ratio and Sweep on Static and Yawing Stability Derivatives of Untapered Wings. NACA TN 1669, 1948.

7. Goodman, Alex, and Adair, Glenn H.: Estimation of the Damping in Roll of Wings through the Normal Flight Range of Lift Coefficient. NACA TN 1924, 1949.

8. Weick, Fred E., and Jones, Robert T.: Résumé and Analysis of N.A.C.A. Lateral Control Research. NACA Rep. 605, 1937.

9. Lowry, John G., and Schneiter, Leslie E.: Estimation of Effectiveness of Flap-Type Controls on Sweptback Wings. NACA TN 1674, 1948.

10. DeYoung, John: Theoretical Antisymmetric Span Loading for Wings of Arbitrary Plan Form at Subsonic Speeds. NACA TN 2140, 1950.

11. DeYoung, John: Spanwise Loading for Wings and Control Surfaces of Low Aspect Ratio. NACA TN 2011, 1950.

12. Dods, Jules B., Jr.: Wind-Tunnel Investigation of Horizontal Tails. IV - Unswept Plan Form of Aspect Ratio 2 and a Two-Dimensional Model. NACA RM A8J21, 1948.

TABLE I.- GEOMETRIC CHARACTERISTICS OF UNTAPERED UNSWEPT LOW-ASPECT-RATIO WING MODELS

[NACA 64A010 airfoil section]

Aspect ratio	Span (ft)	Root chord (ft)	M.A.C. (ft)	Area (sq ft)	Distance from $\bar{c}/4$ to wing leading edge (ft)
6.13	6.100	1.000	0.997	6.067	0.250
4.13	5.021	1.224	1.221	6.097	.306
2.13	3.638	1.732	1.714	6.199	.432
1.13	2.693	2.448	2.409	6.394	.611

NACA

TABLE II.- AILERON CONFIGURATIONS TESTED

Aspect ratio	Aileron location					
	Outboard ailerons			Inboard ailerons		
	Span	$\frac{y_i}{b/2}$	$\frac{y_o}{b/2}$	Span	$\frac{y_i}{b/2}$	$\frac{y_o}{b/2}$
6.13	0.925b/2 .746 .500 .254	0.067 .246 .492 .738	0.992 .992 .992 .992	0.425b/2 .179	0.067 .067	0.492 .246
4.13	.916 .746 .502 .257	.073 .243 .487 .732	.989 .989 .989 .989	.414 .170	.073 .073	.487 .243
2.13	.978 .741 .502 .263	0 .237 .476 .715	.978 .978 .978 .978	.476 .237	0 0	.476 .237
1.13	.957 .729 .502 .275	0 .228 .455 .682	.957 .957 .957 .957	.455 .228	0 0	.455 .228

NACA

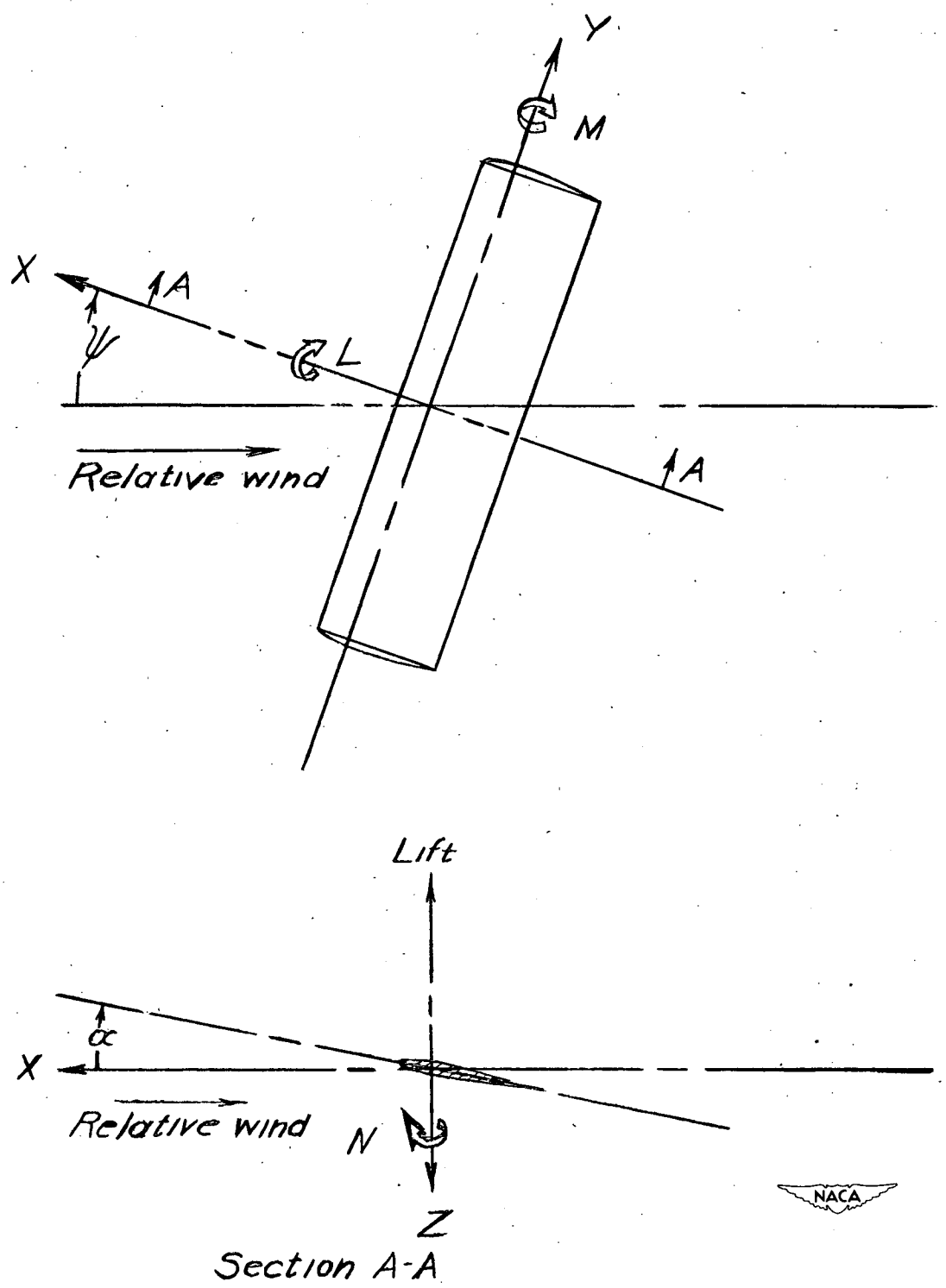

Figure 1.- System of stability axes. Positive values of forces, moments, and angles are indicated by arrows.

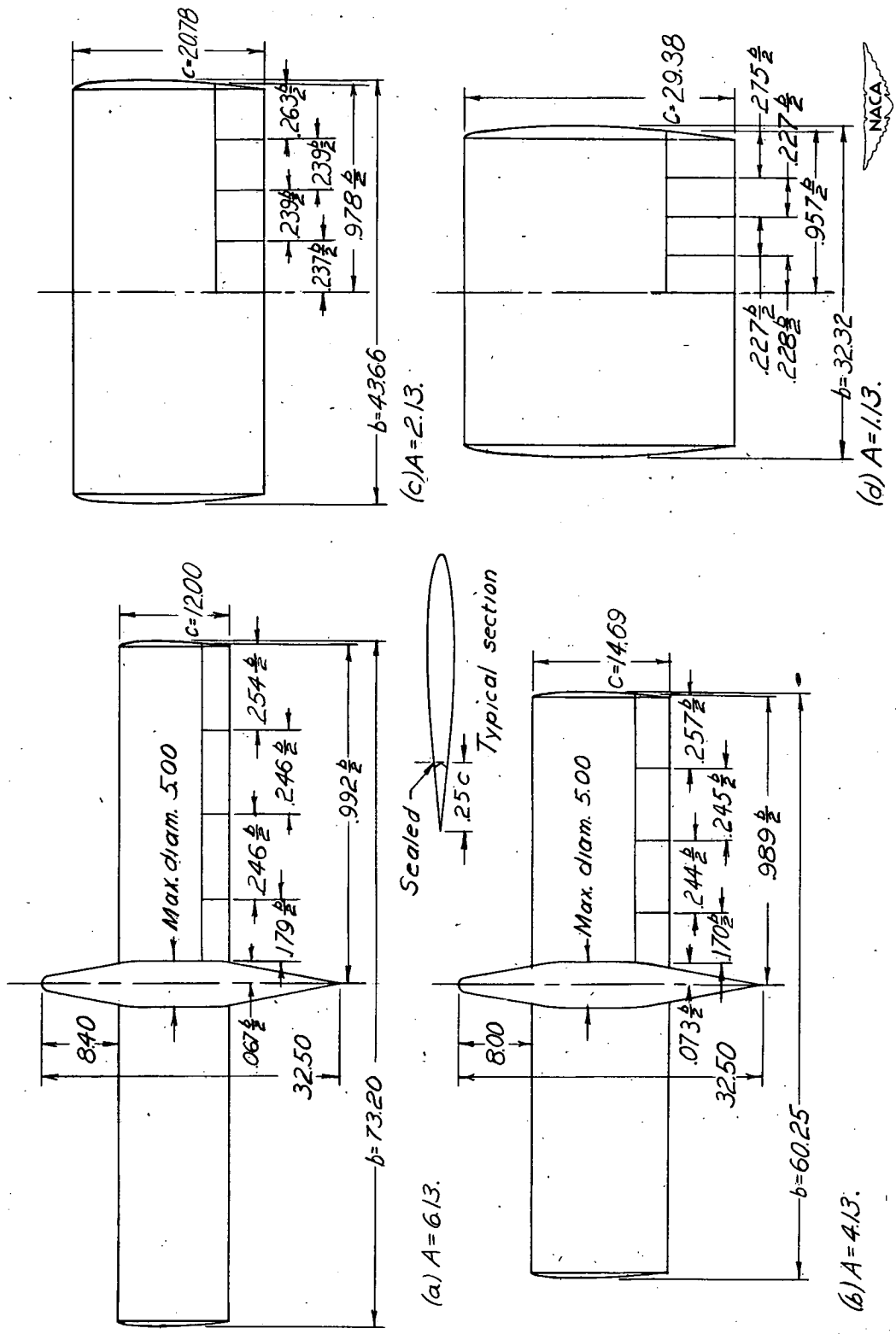

Figure 2.- Geometry of the models. All dimensions are in inches.

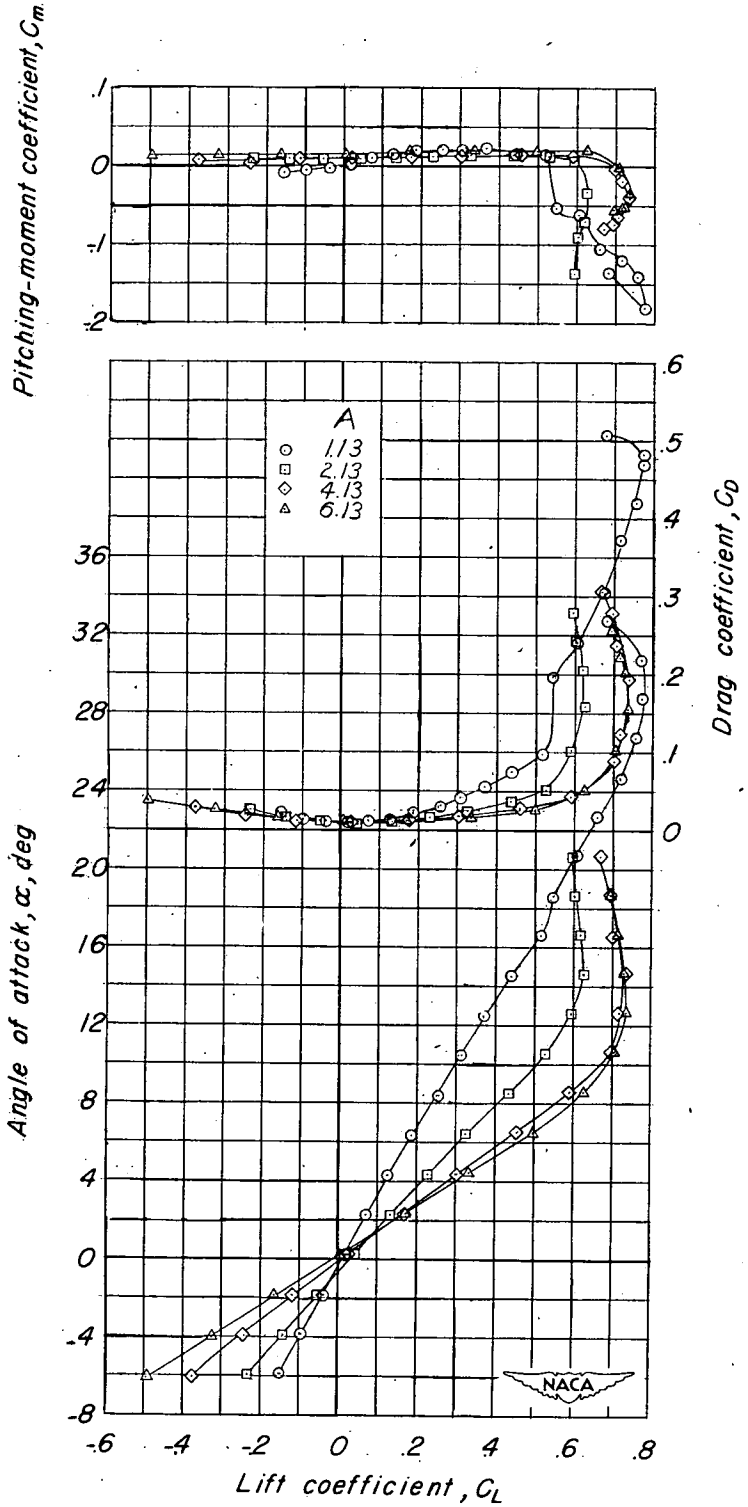

Figure 3.- Aerodynamic characteristics in pitch of the wings. $\delta_a = 0°$; $\psi = 0°$.

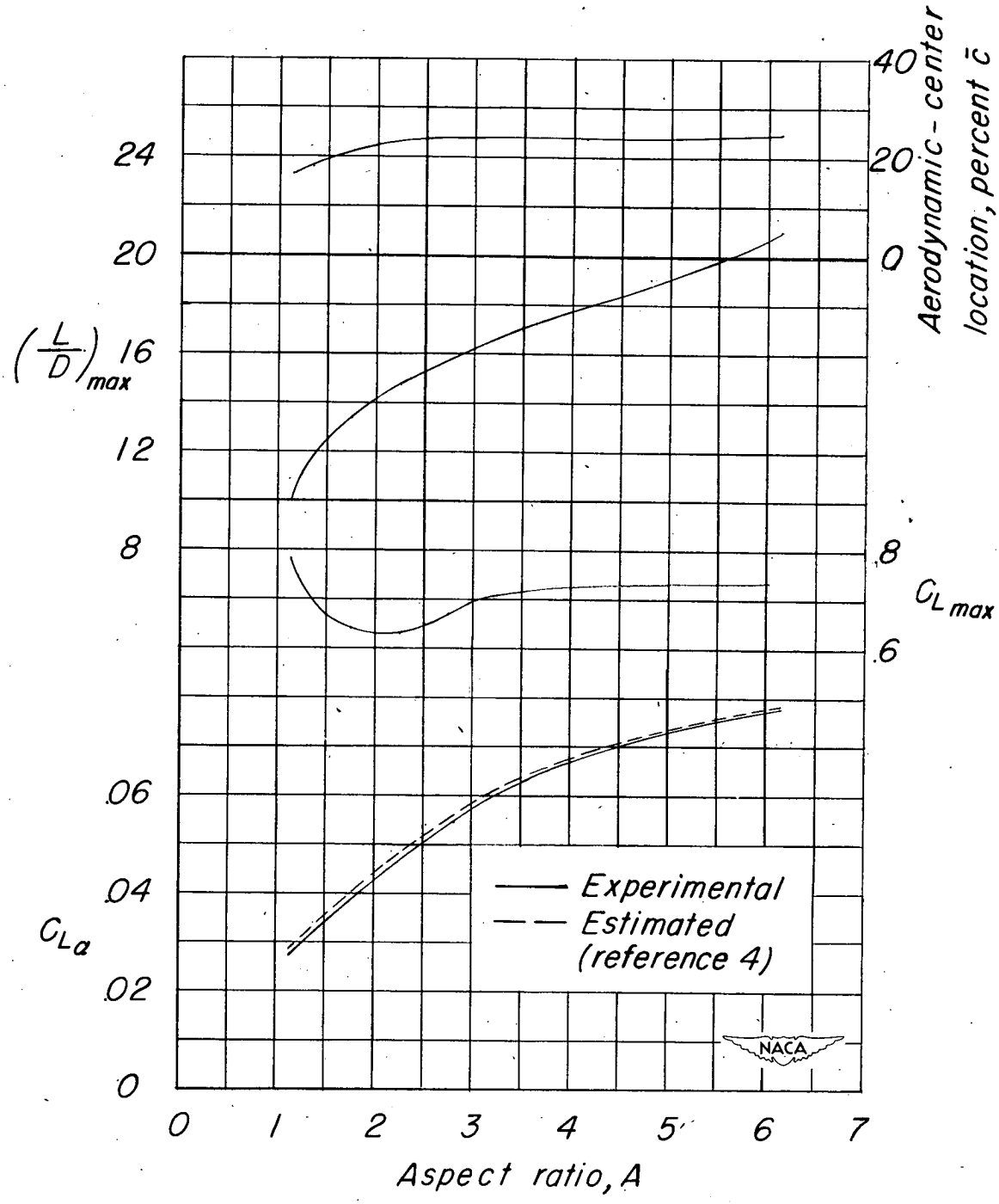

Figure 4.- Variation of C_{L_α}, $C_{L_{max}}$, $(L/D)_{max}$, and aerodynamic-center location with aspect ratio.

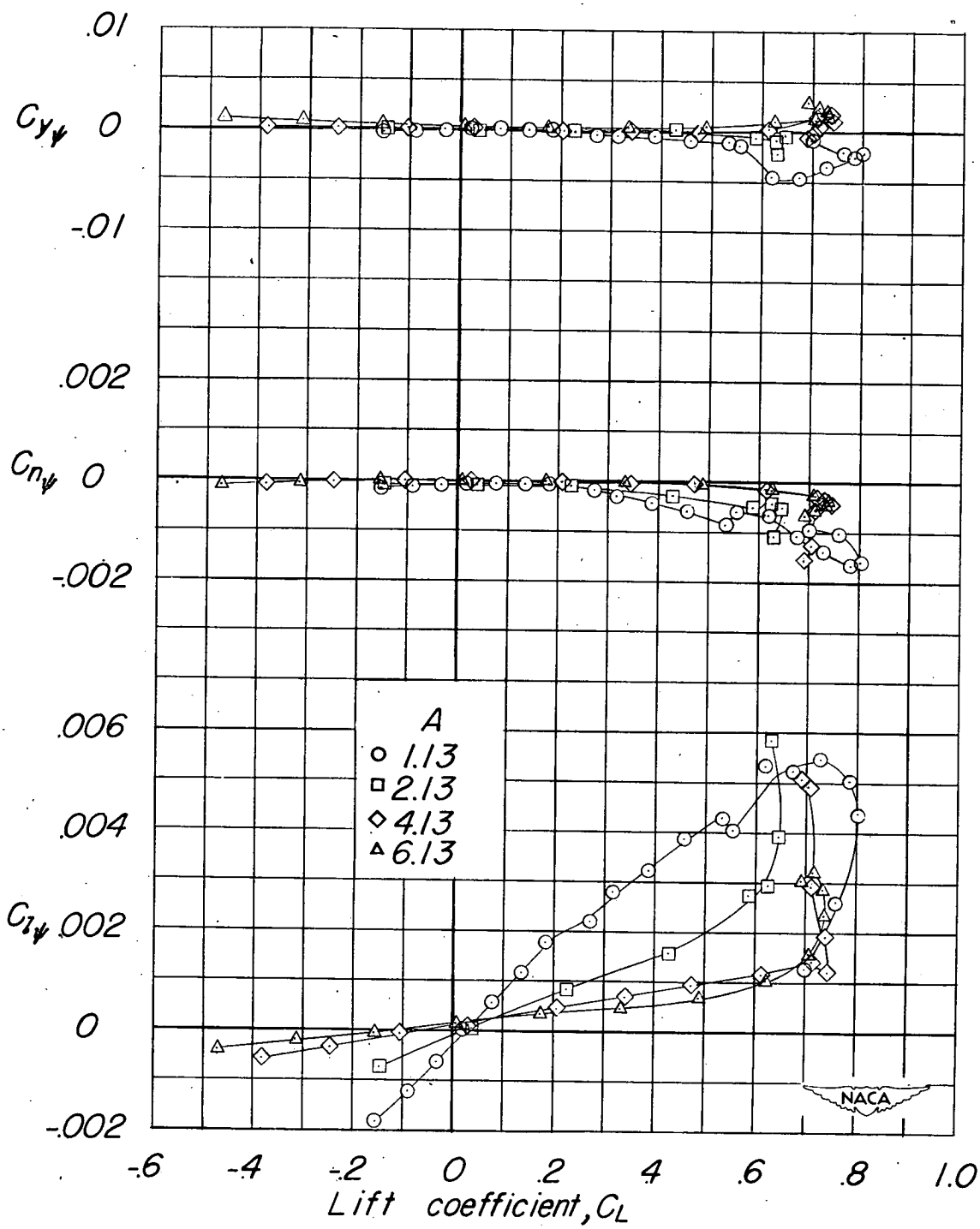

Figure 5.- Variation of the derivatives C_{l_ψ}, C_{n_ψ}, and C_{Y_ψ} with lift coefficient. $\delta_a = 0^\circ$.

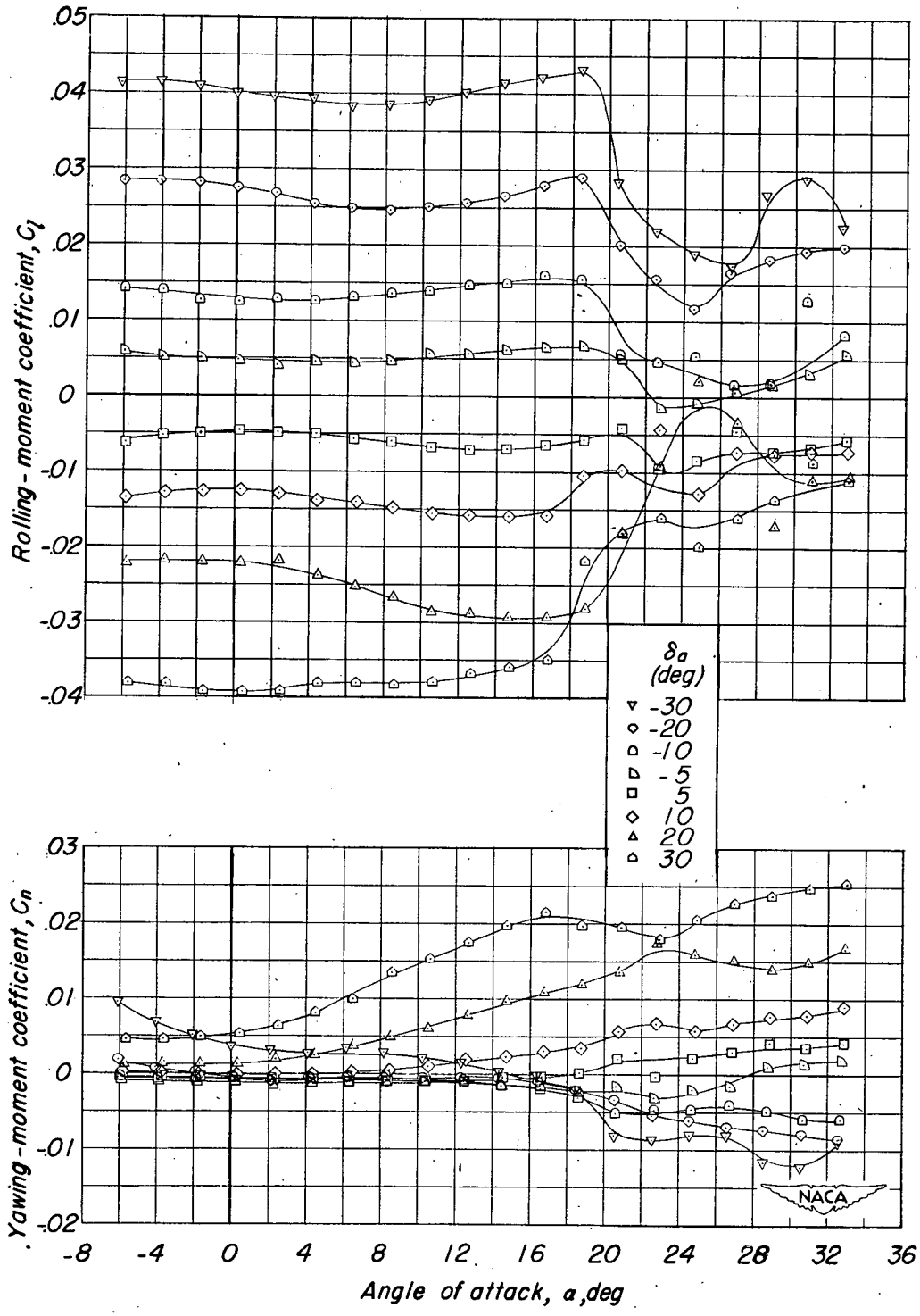

Figure 6.- Variation of the lateral control characteristics of the A = 1.13 wing with angle of attack. Outboard ailerons; $\frac{b_a}{b/2} = 0.957$.

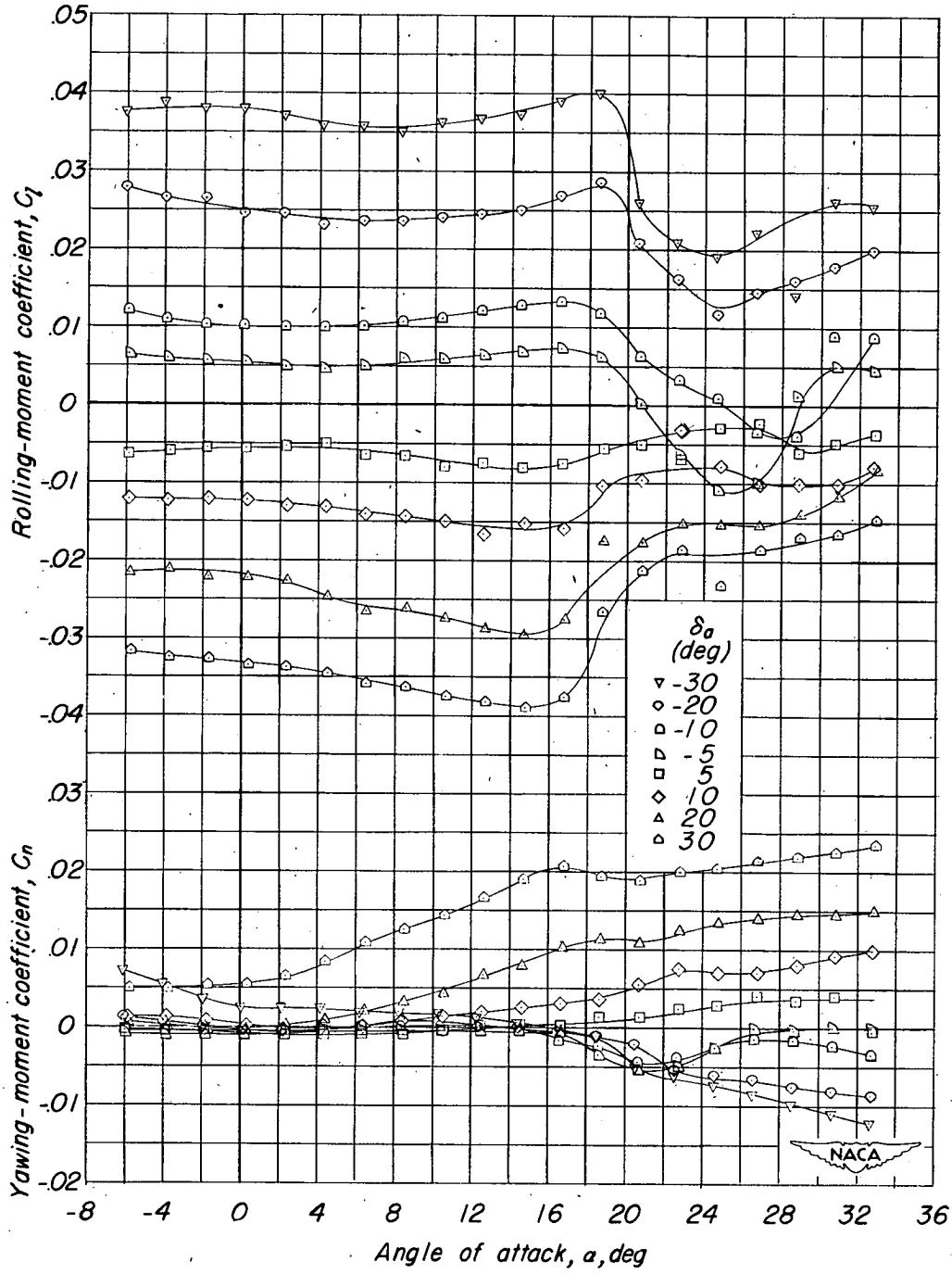

Figure 7.- Variation of the lateral control characteristics of the A = 1.13 wing with angle of attack. Outboard ailerons; $\frac{b_a}{b/2} = 0.729$.

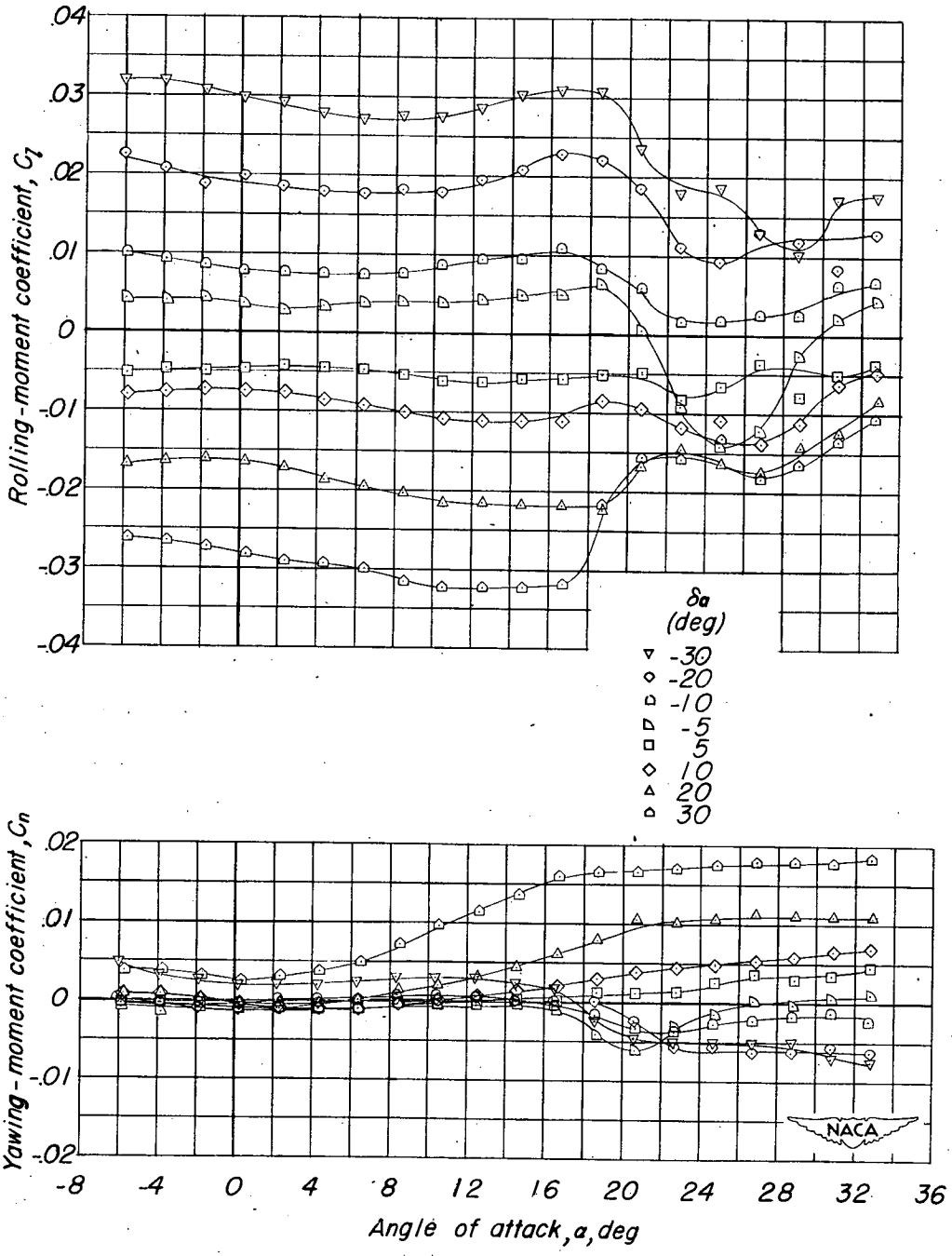

Figure 8.- Variation of the lateral control characteristics of the A = 1.13 wing with angle of attack. Outboard ailerons; $\frac{b_a}{b/2} = 0.502$.

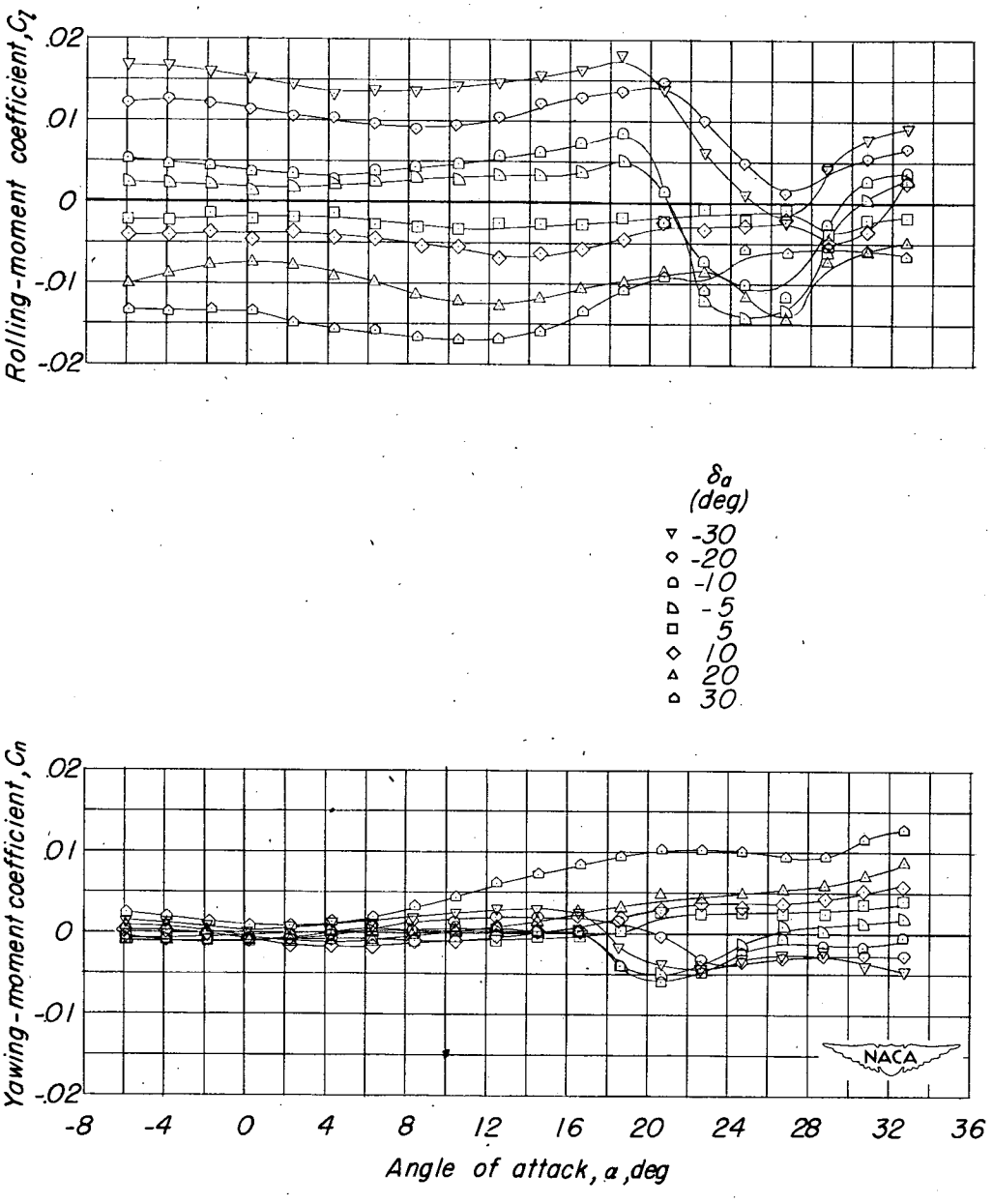

Figure 9.- Variation of the lateral control characteristics of the A = 1.13 wing with angle of attack. Outboard ailerons; $\frac{b_a}{b/2} = 0.275$.

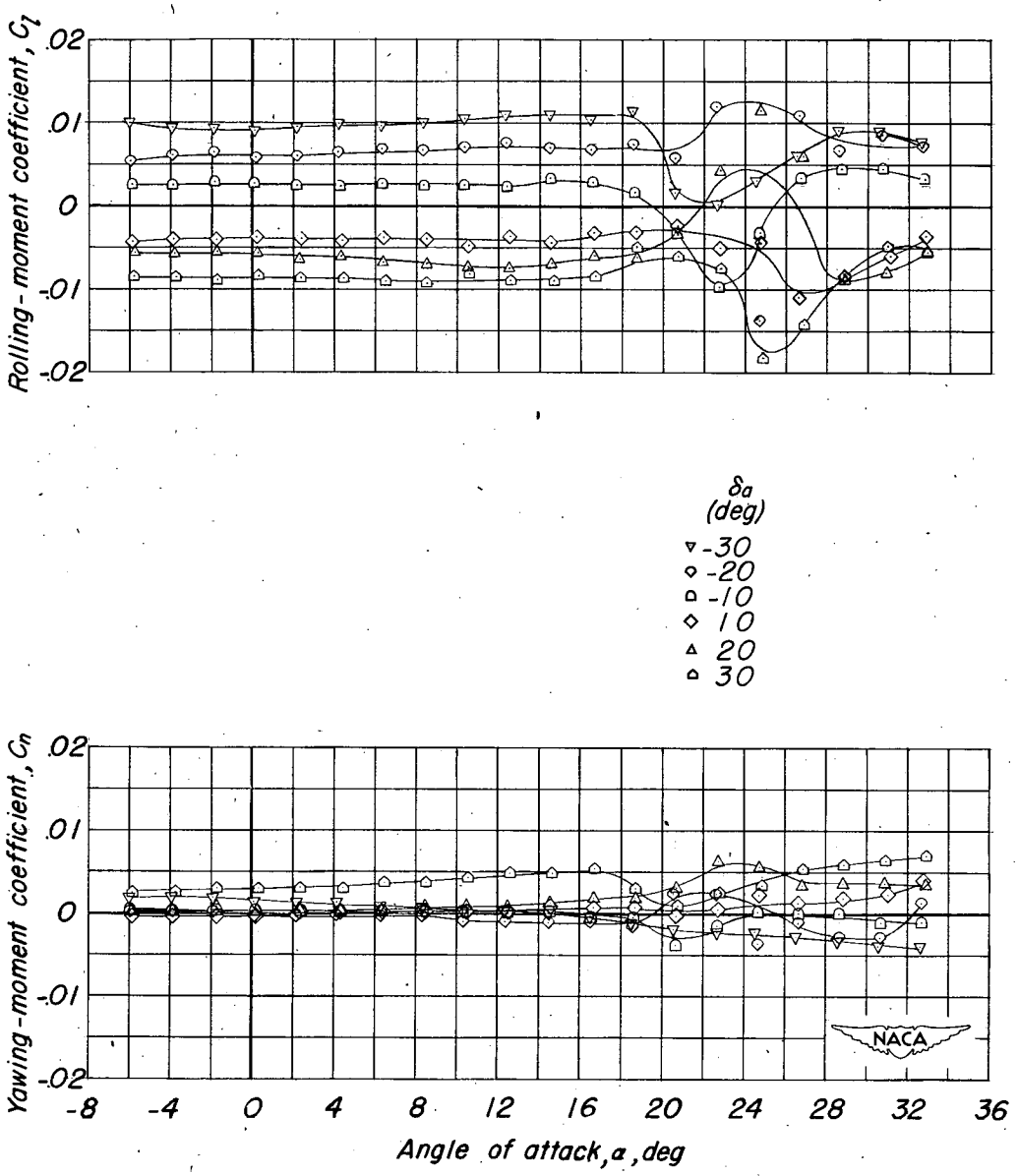

Figure 10.- Variation of the lateral control characteristics of the A = 1.13 wing with angle of attack. Inboard ailerons; $\frac{b_a}{b/2} = 0.455$.

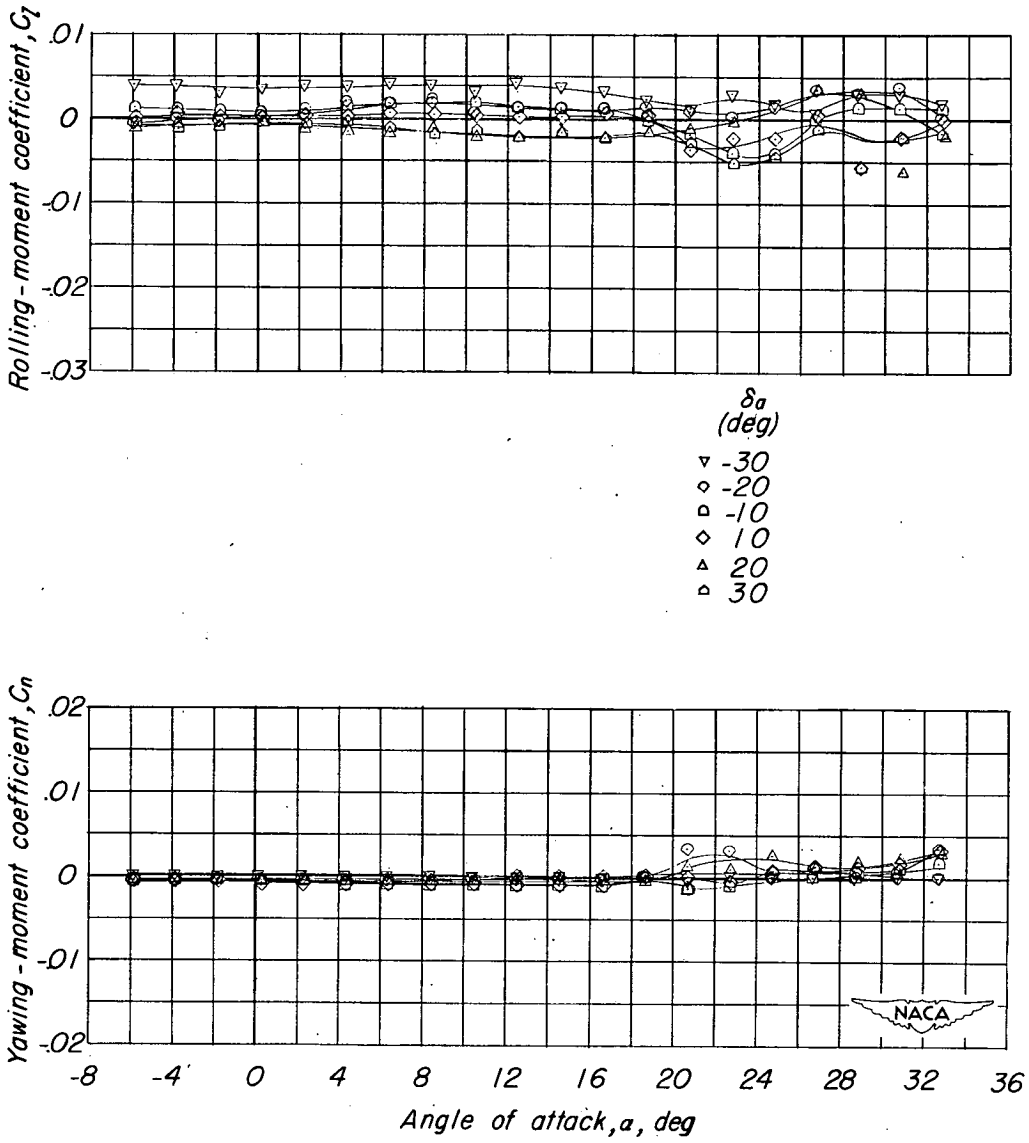

Figure 11.- Variation of the lateral control characteristics of the A = 1.13 wing with angle of attack. Inboard ailerons; $\frac{b_a}{b/2} = 0.228$.

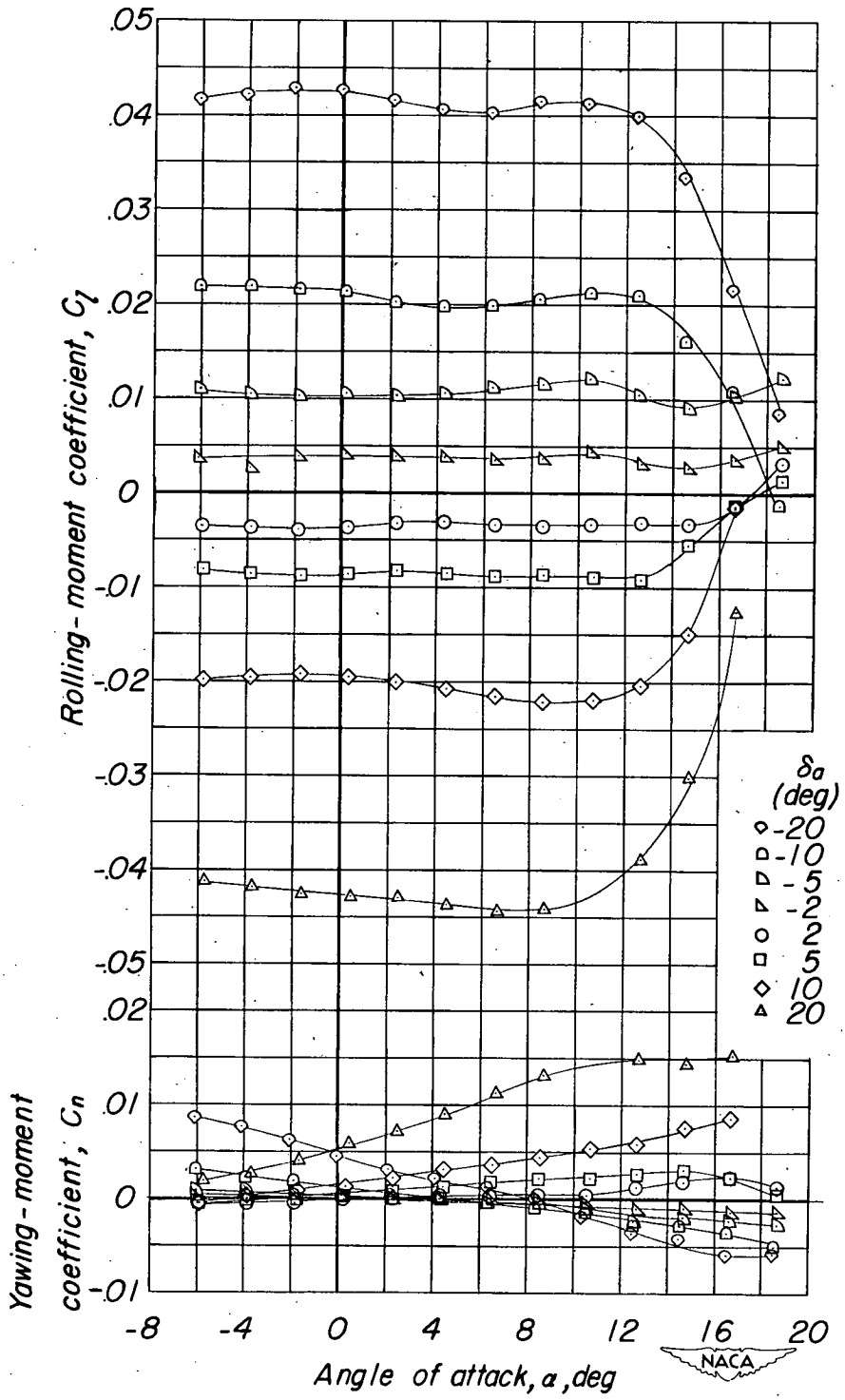

Figure 12.- Variation of the lateral control characteristics of the A = 2.13 wing with angle of attack. Outboard ailerons; $\frac{b_a}{b/2} = 0.978$.

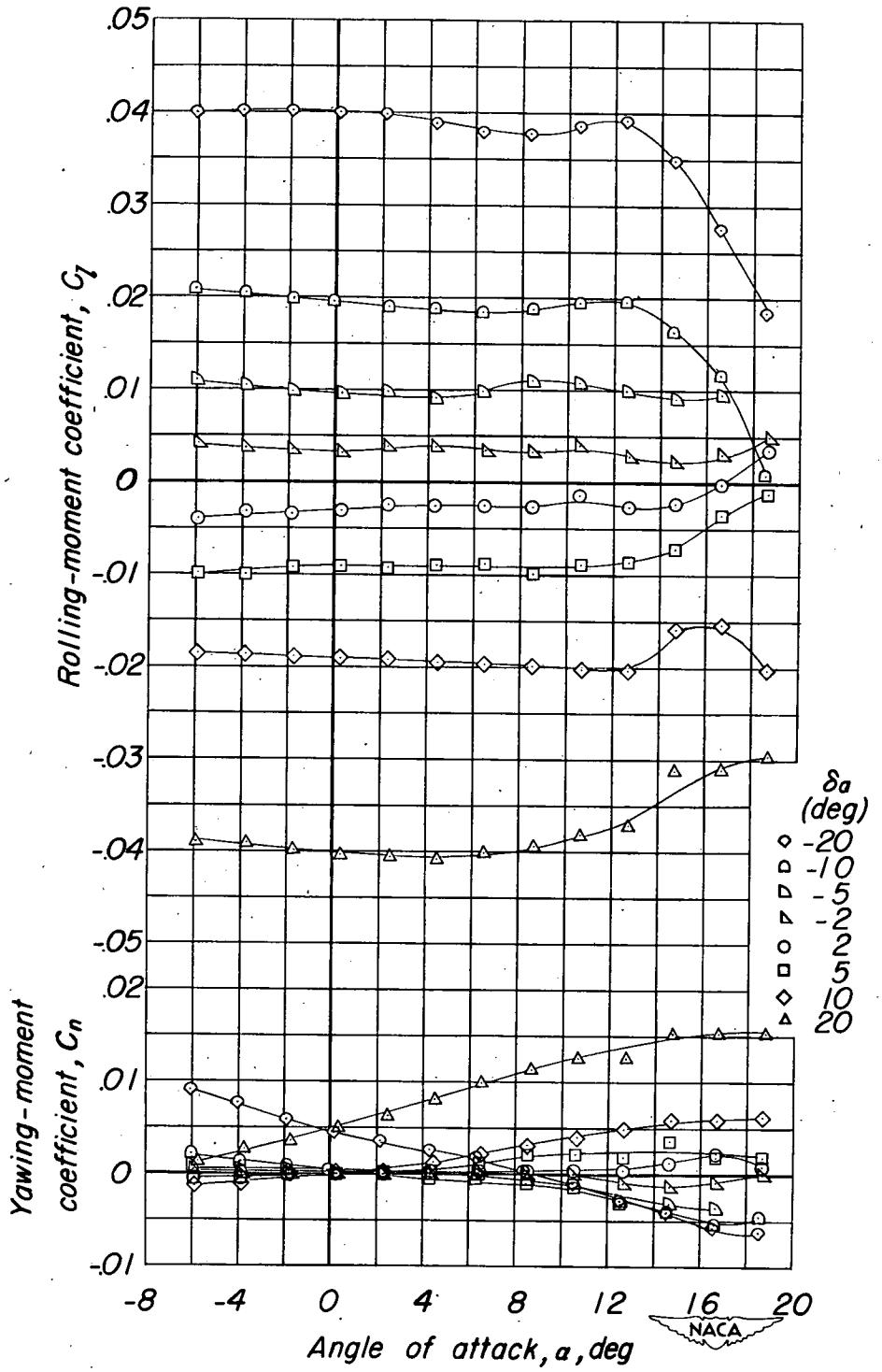

Figure 13.- Variation of the lateral control characteristics of the A = 2.13 wing with angle of attack. Outboard ailerons; $\frac{b_a}{b/2} = 0.741$.

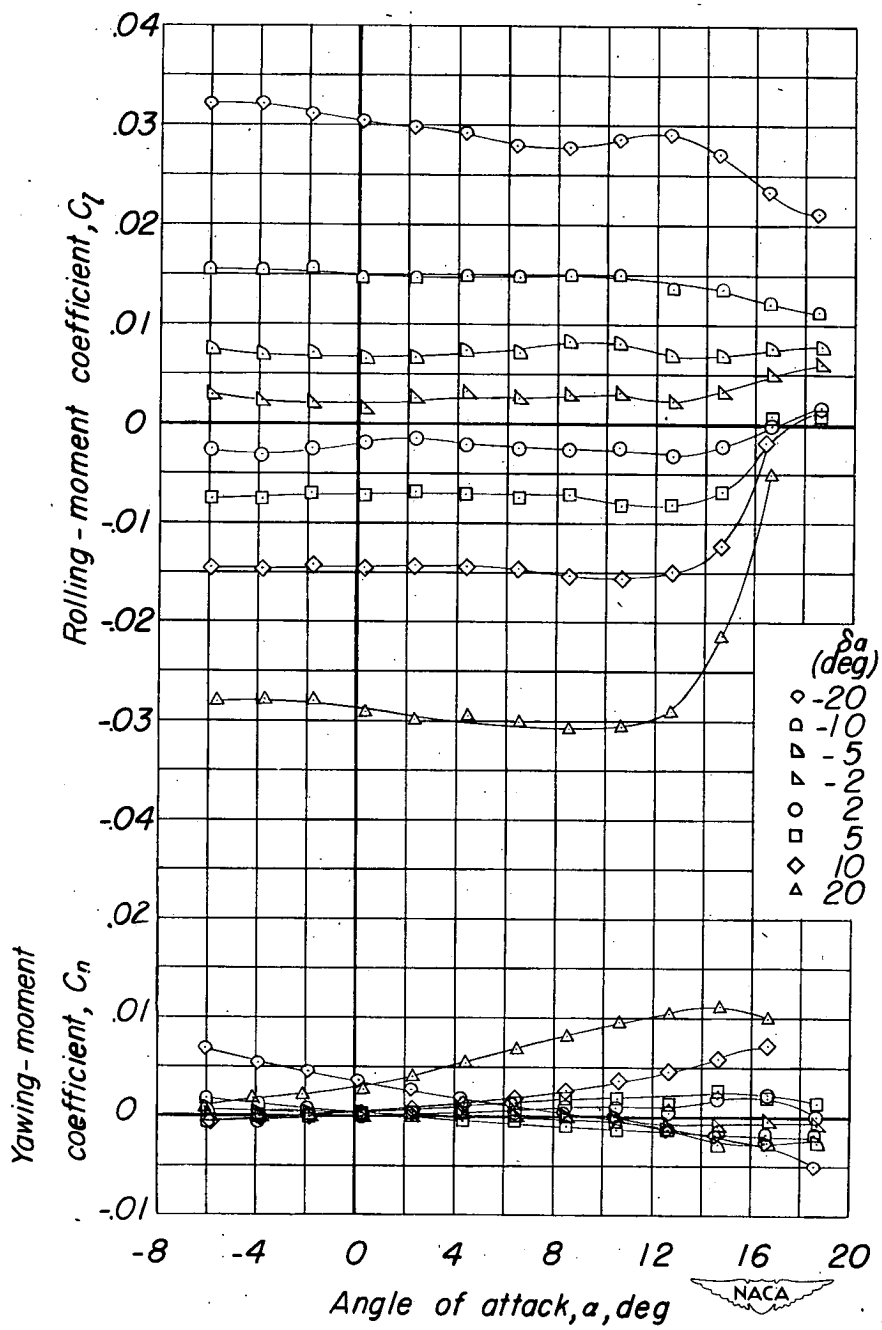

Figure 14.- Variation of the lateral control characteristics of the A = 2.13 wing with angle of attack. Outboard ailerons; $\frac{b_a}{b/2} = 0.502$.

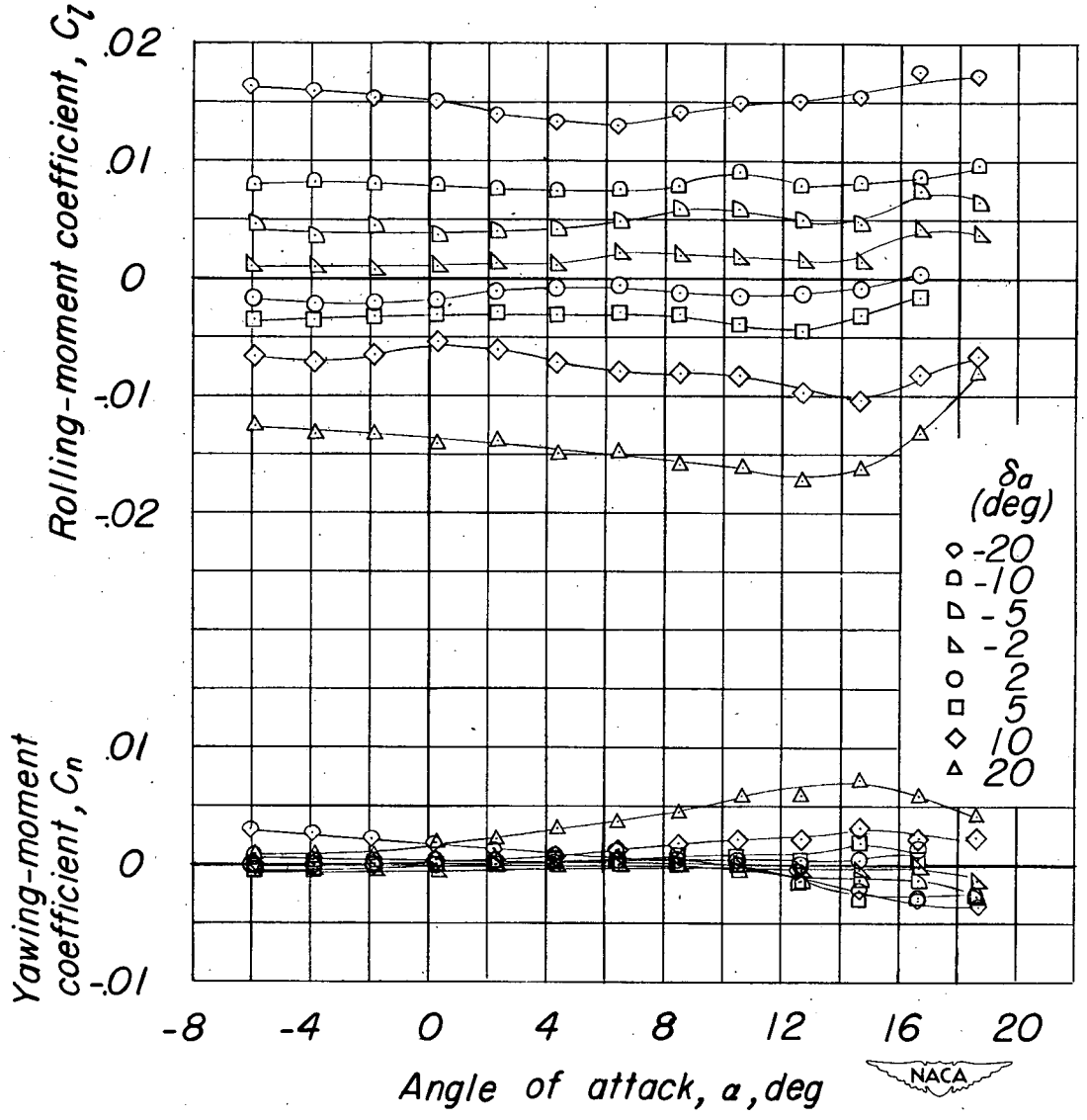

Figure 15.- Variation of the lateral control characteristics of the A = 2.13 wing with angle of attack. Outboard ailerons; $\frac{b_a}{b/2}$ = 0.263.

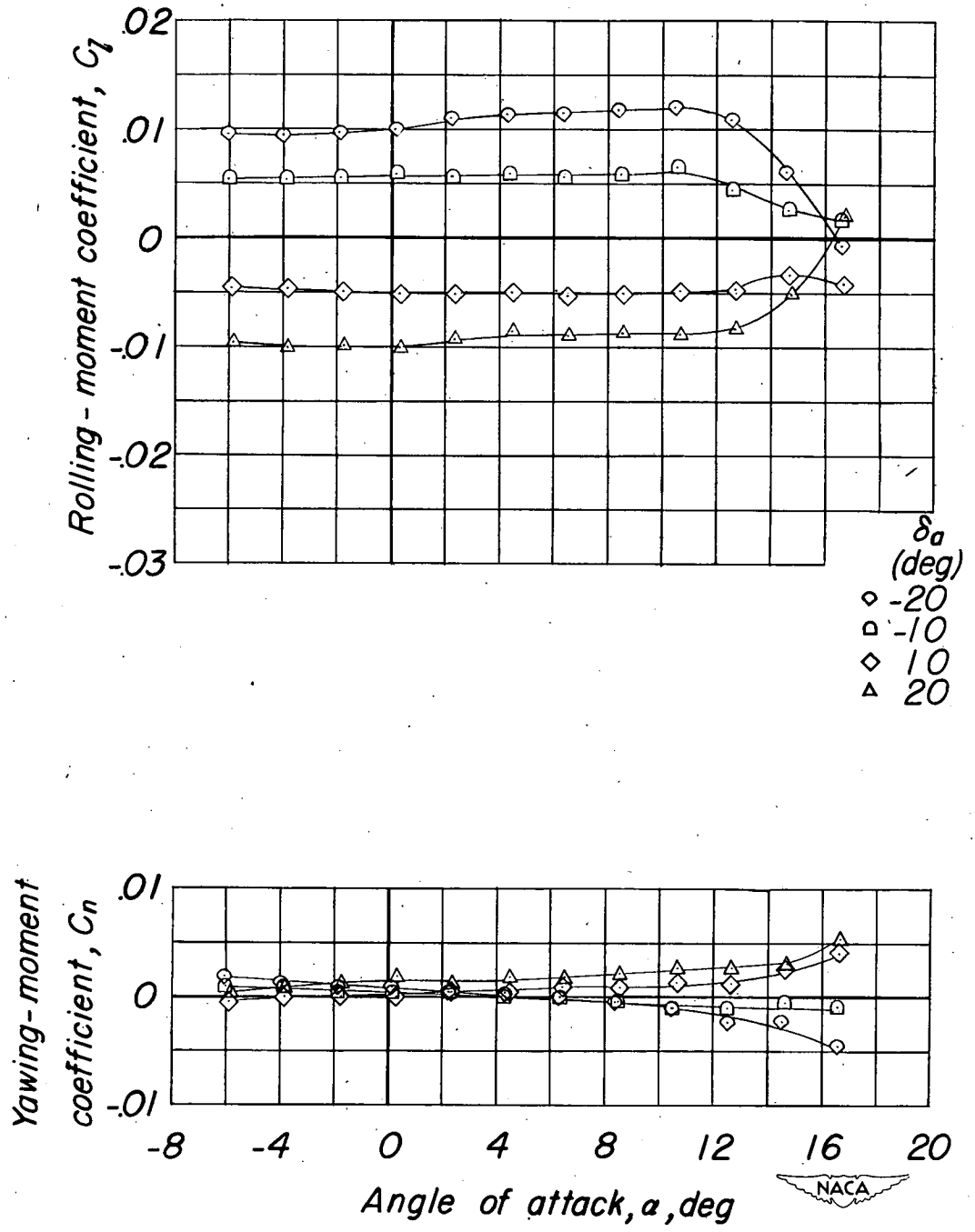

Figure 16.- Variation of the lateral control characteristics of the A = 2.13 wing with angle of attack. Inboard ailerons; $\frac{b_a}{b/2} = 0.476$.

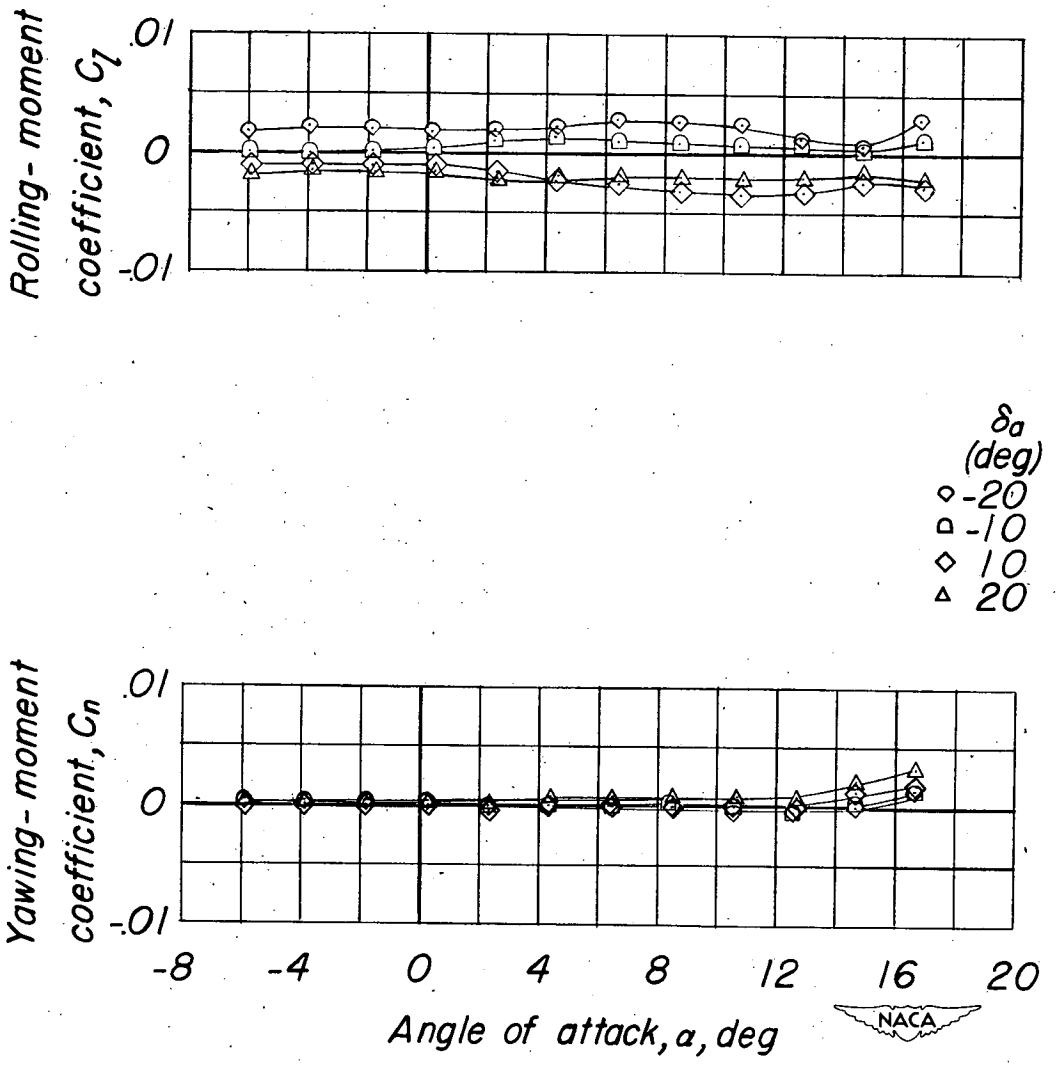

Figure 17.- Variation of the lateral control characteristics of the A = 2.13 wing with angle of attack. Inboard ailerons; $\frac{b_a}{b/2}$ = 0.237.

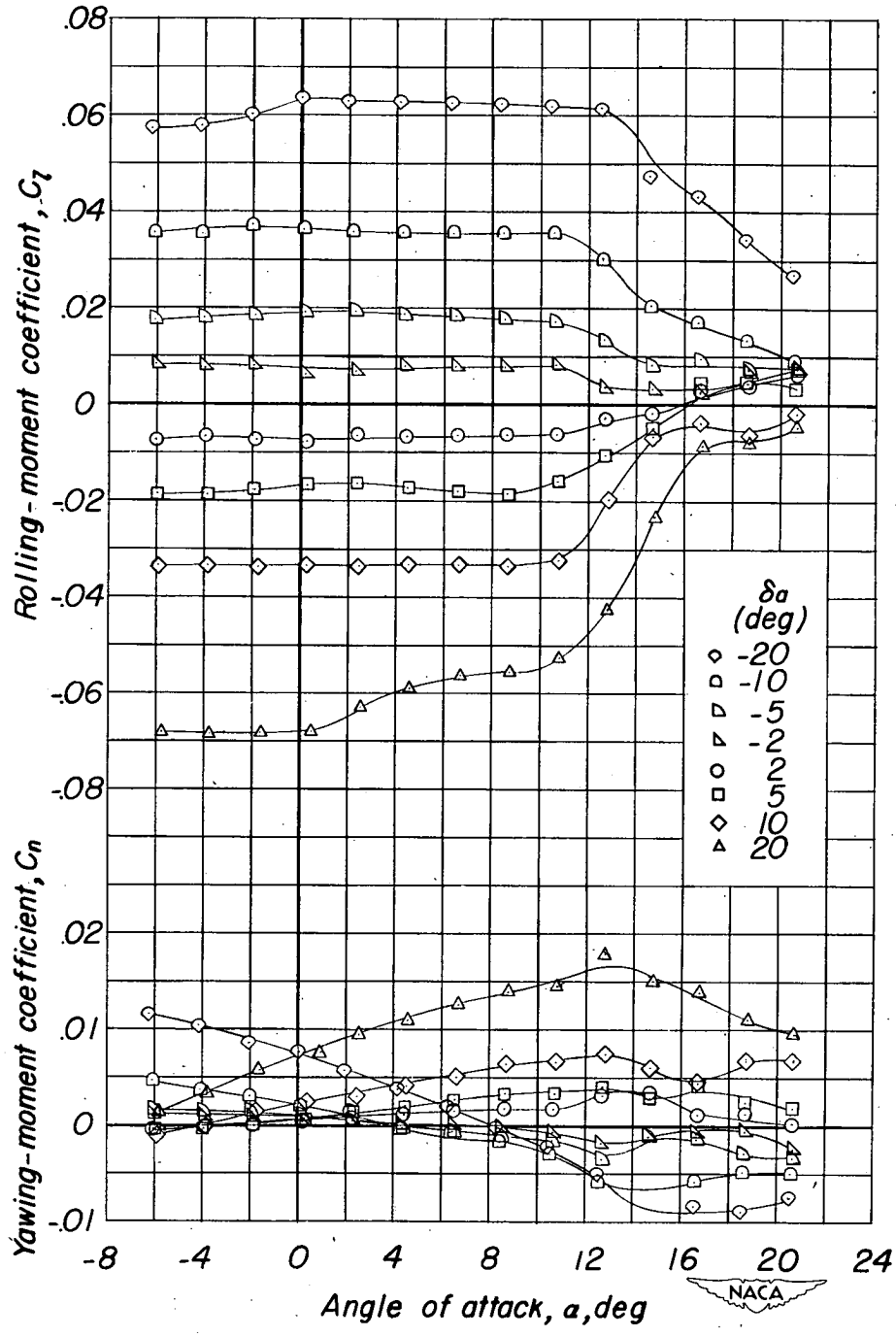

Figure 18.- Variation of the lateral control characteristics of the A = 4.13 wing with angle of attack. Outboard ailerons; $\frac{b_a}{b/2} = 0.916$.

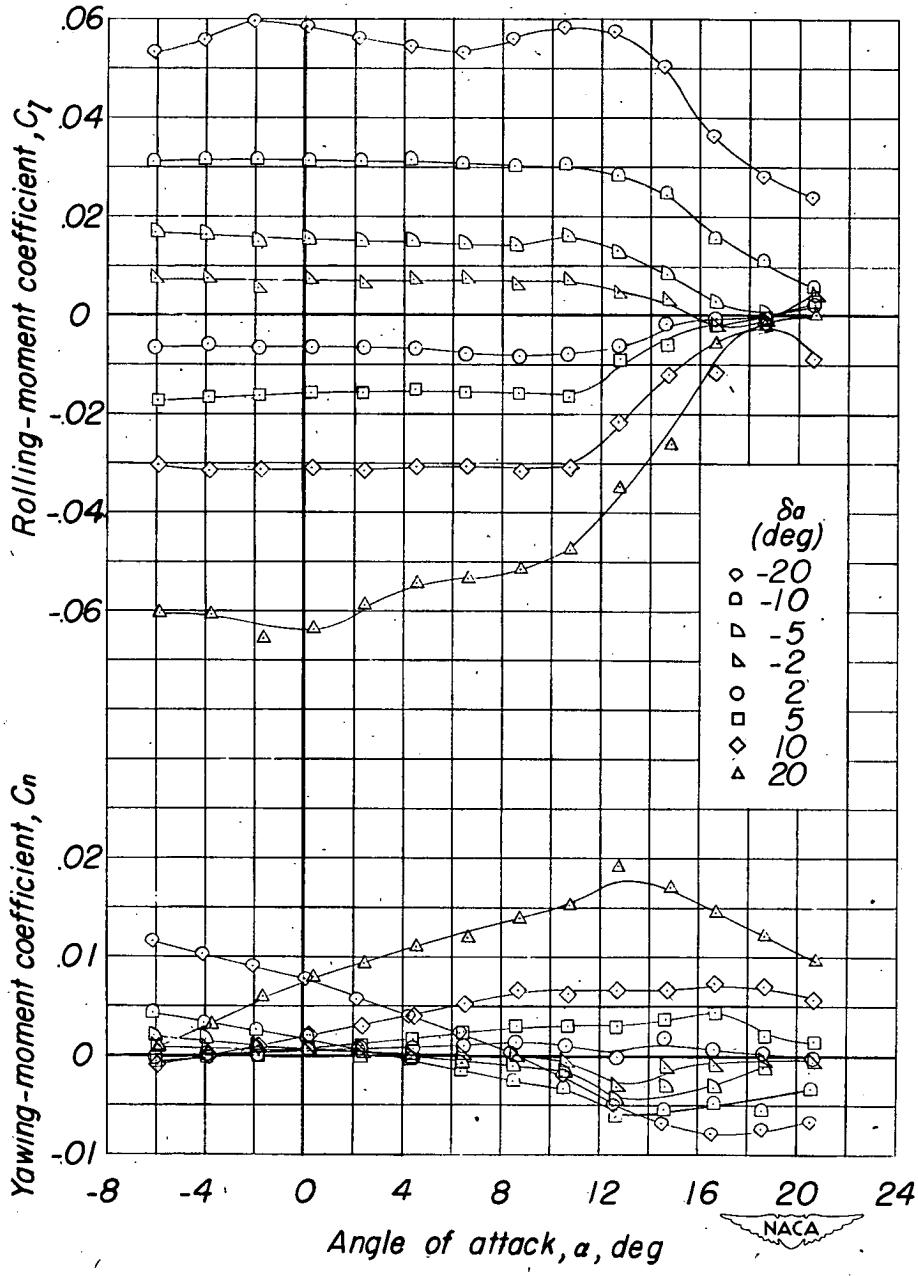

Figure 19.- Variation of the lateral control characteristics of the A = 4.13 wing with angle of attack. Outboard ailerons; $\frac{b_a}{b/2} = 0.746$.

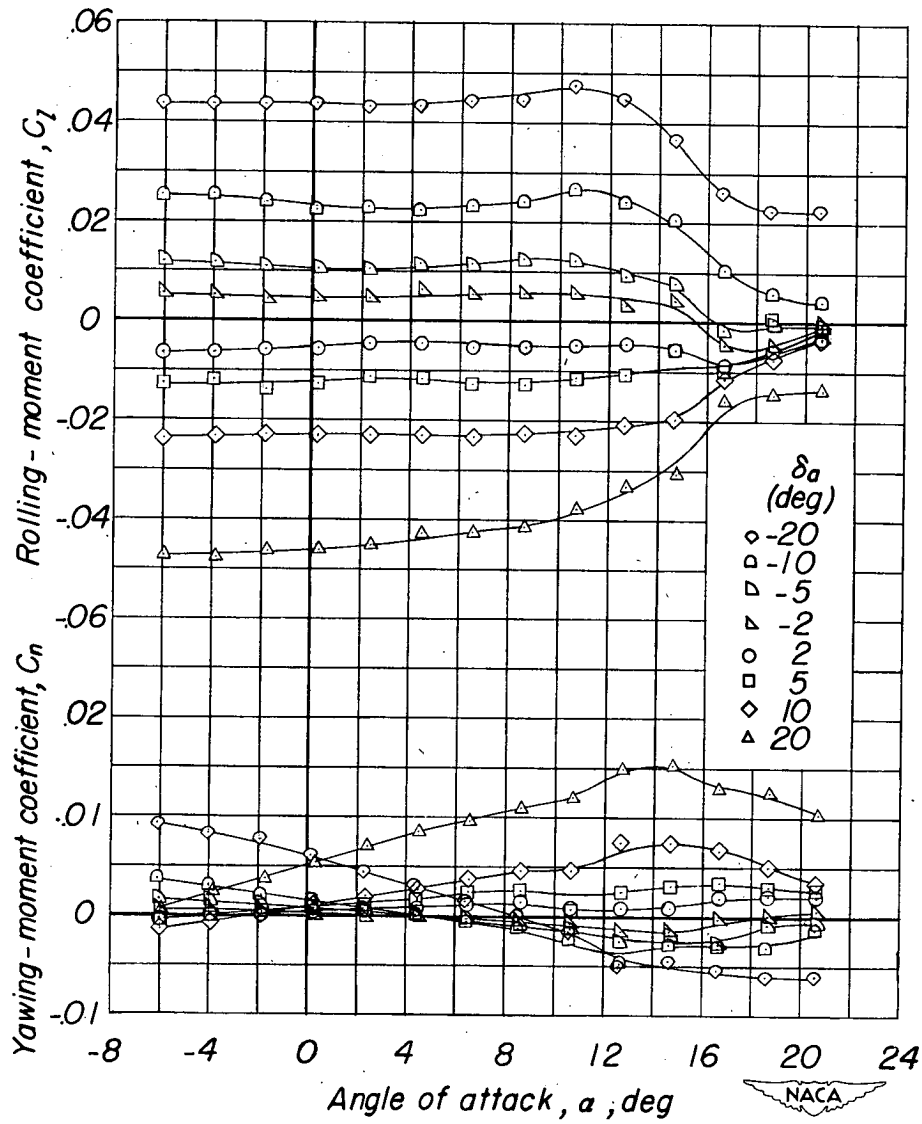

Figure 20.- Variation of the lateral control characteristics of the A = 4.13 wing with angle of attack. Outboard ailerons; $\frac{b_a}{b/2} = 0.502$.

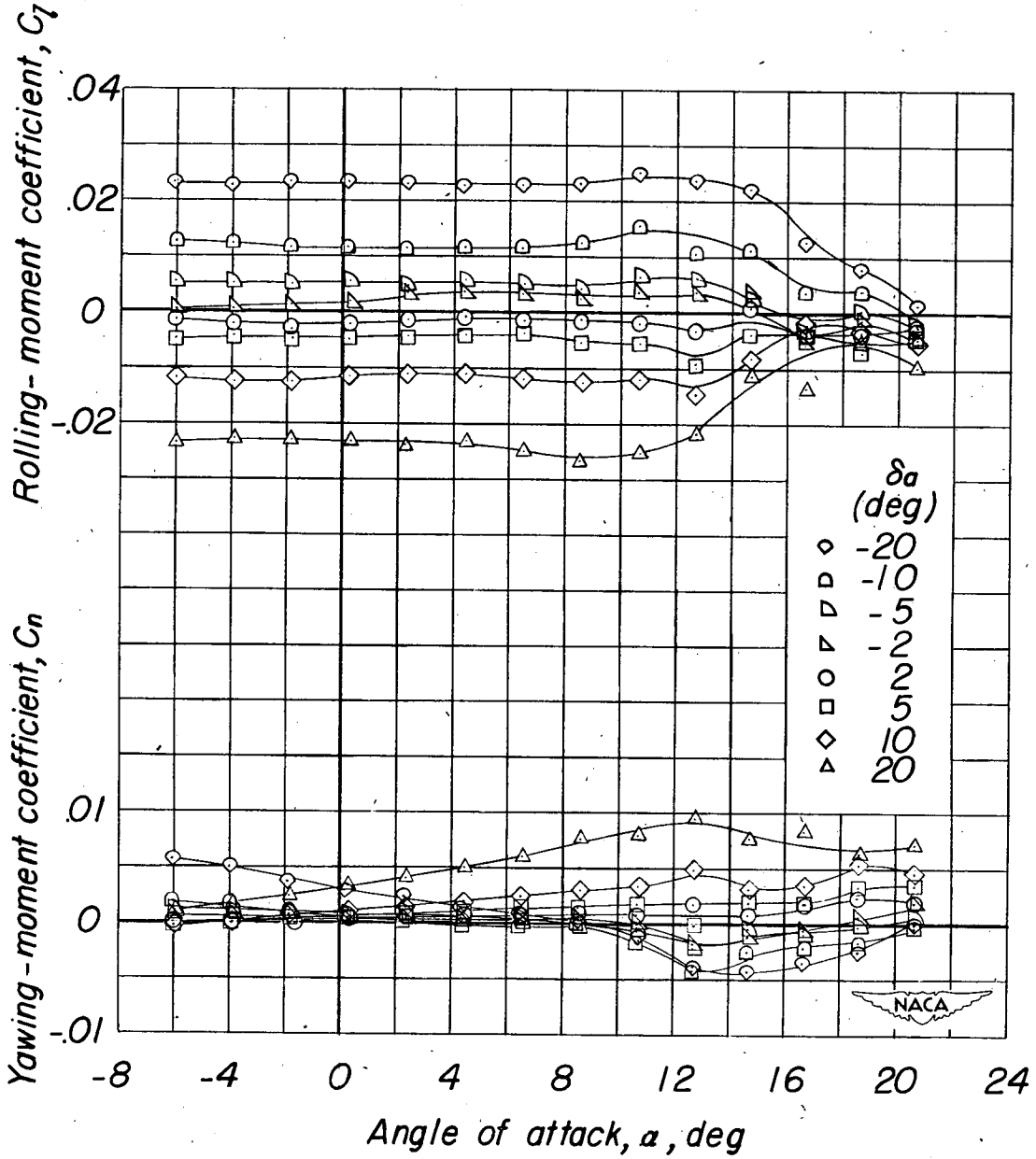

Figure 21.- Variation of the lateral control characteristics of the A = 4.13 wing with angle of attack. Outboard ailerons; $\frac{b_a}{b/2} = 0.257$.

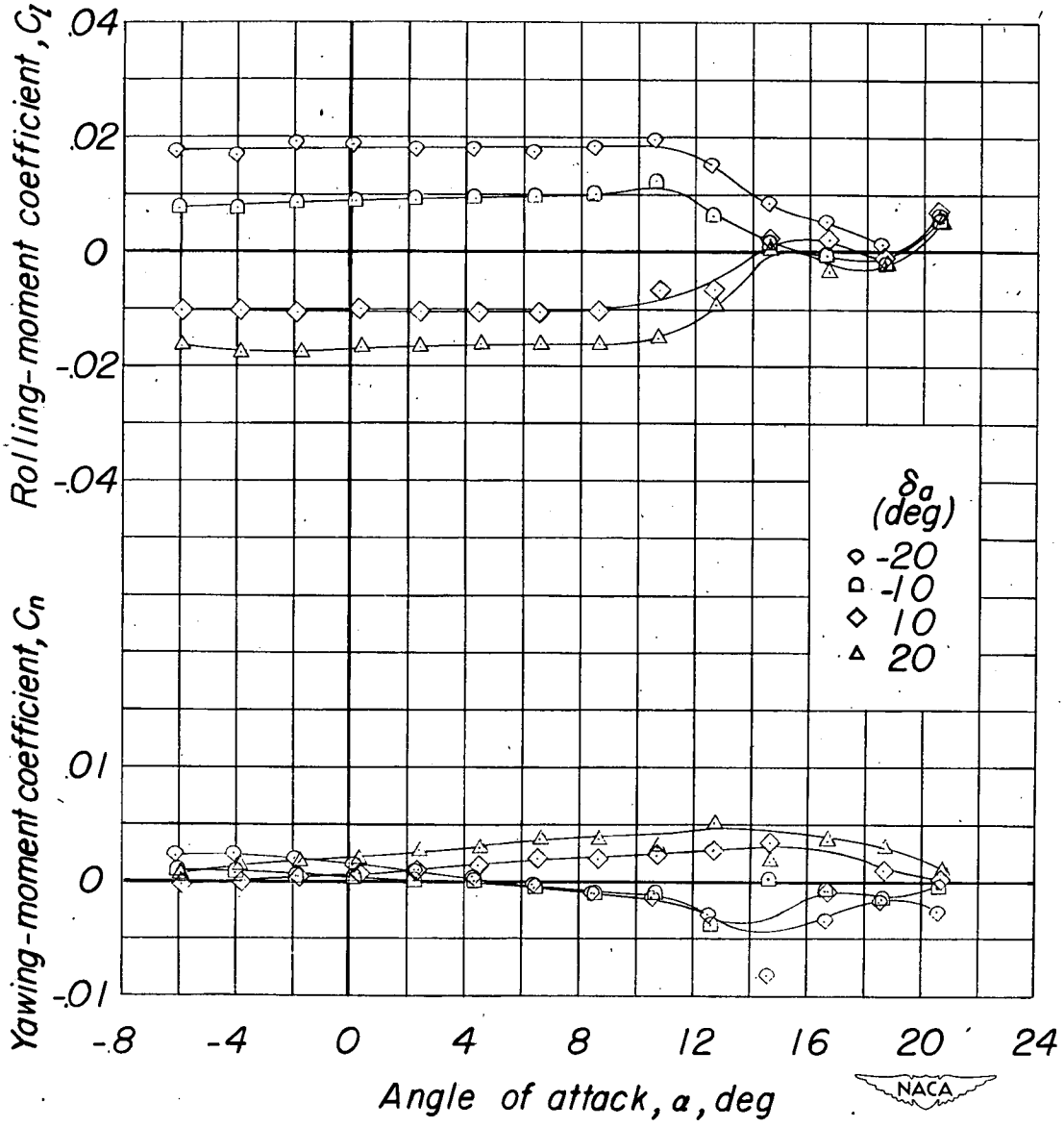

Figure 22.- Variation of the lateral control characteristics of the A = 4.13 wing with angle of attack. Inboard ailerons; $\frac{b_a}{b/2} = 0.414$.

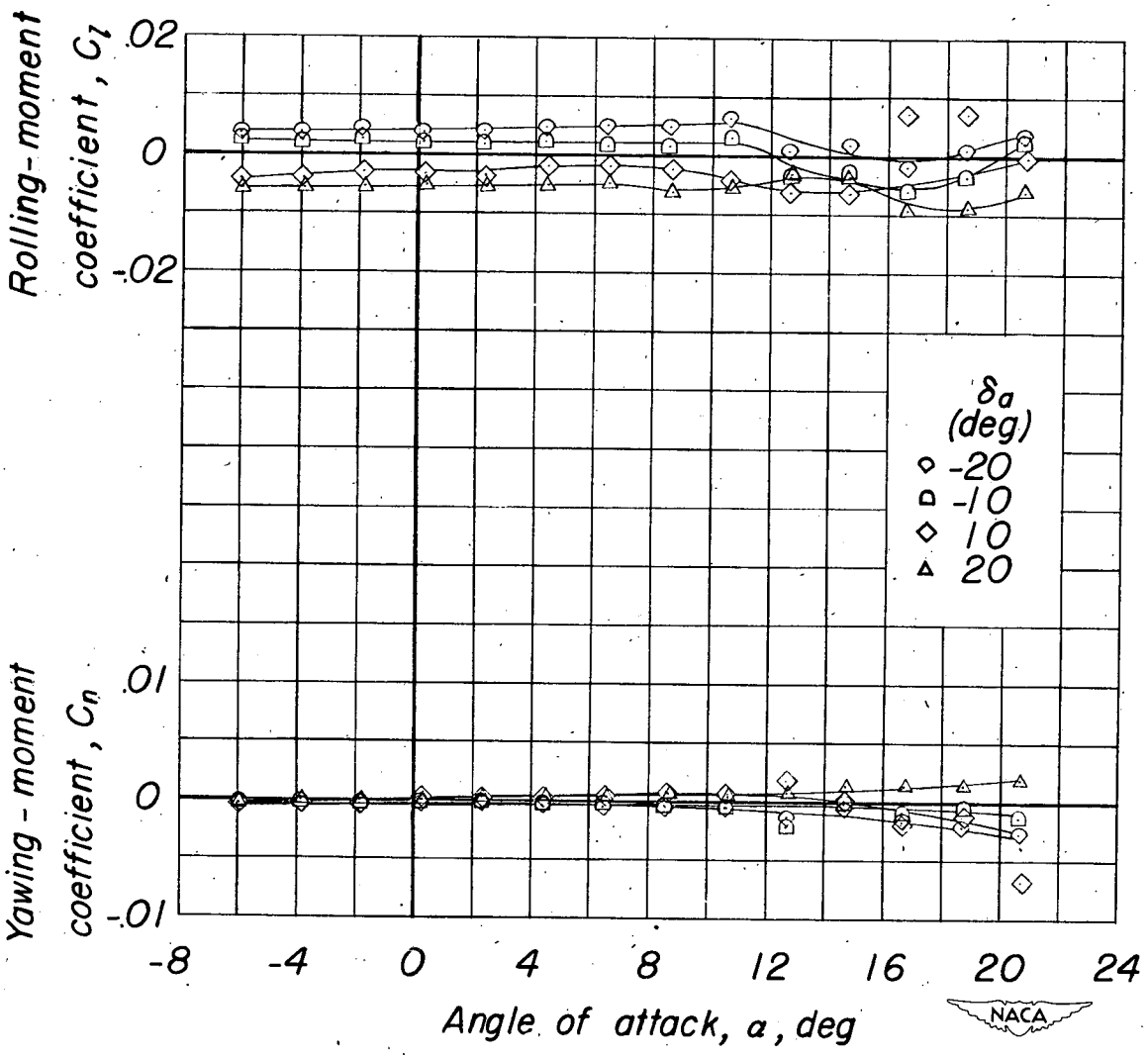

Figure 23.- Variation of the lateral control characteristics of the A = 4.13 wing with angle of attack. Inboard ailerons; $\frac{b_a}{b/2} = 0.170$.

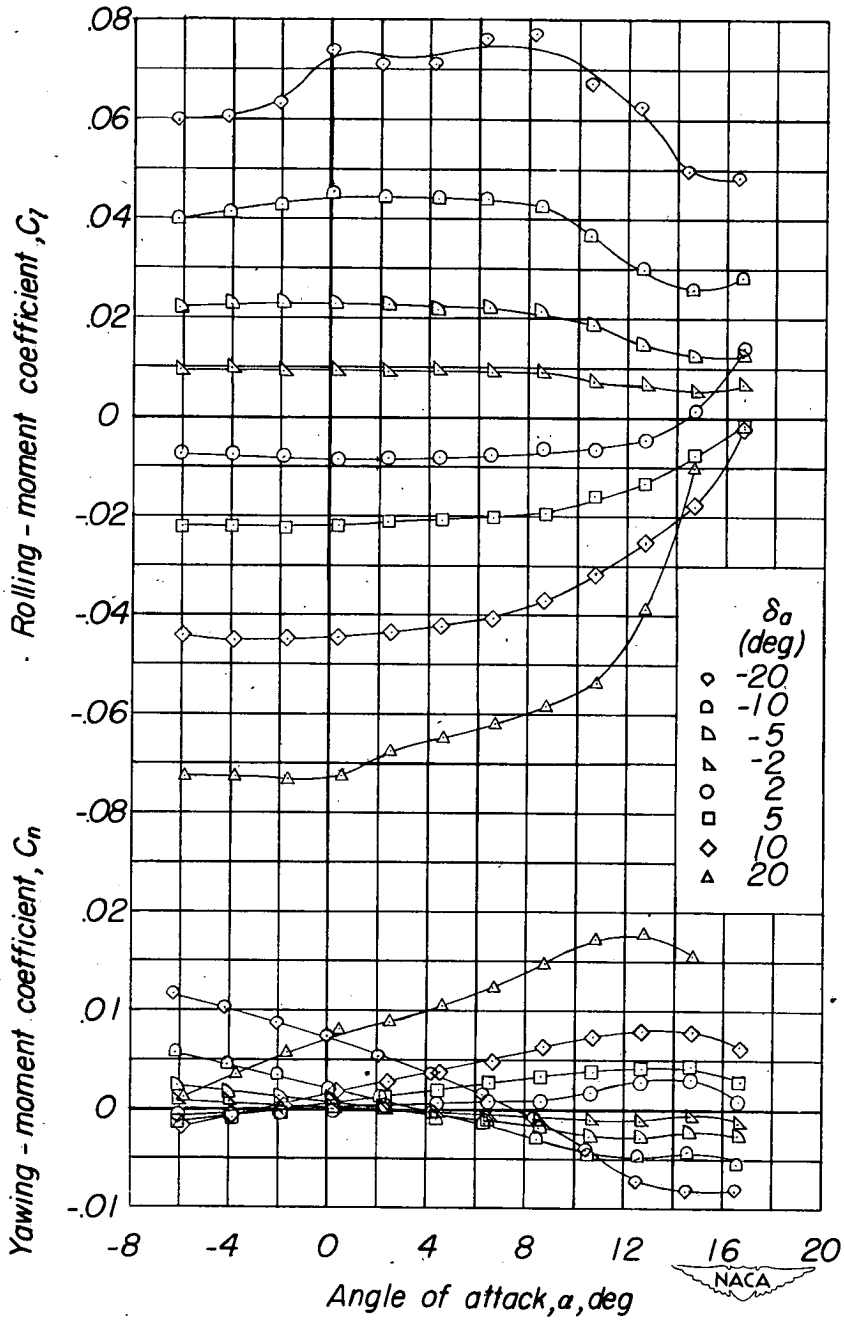

Figure 24.- Variation of the lateral control characteristics of the $A = 6.13$ wing with angle of attack. Outboard ailerons; $\frac{b_a}{b/2} = 0.925$.

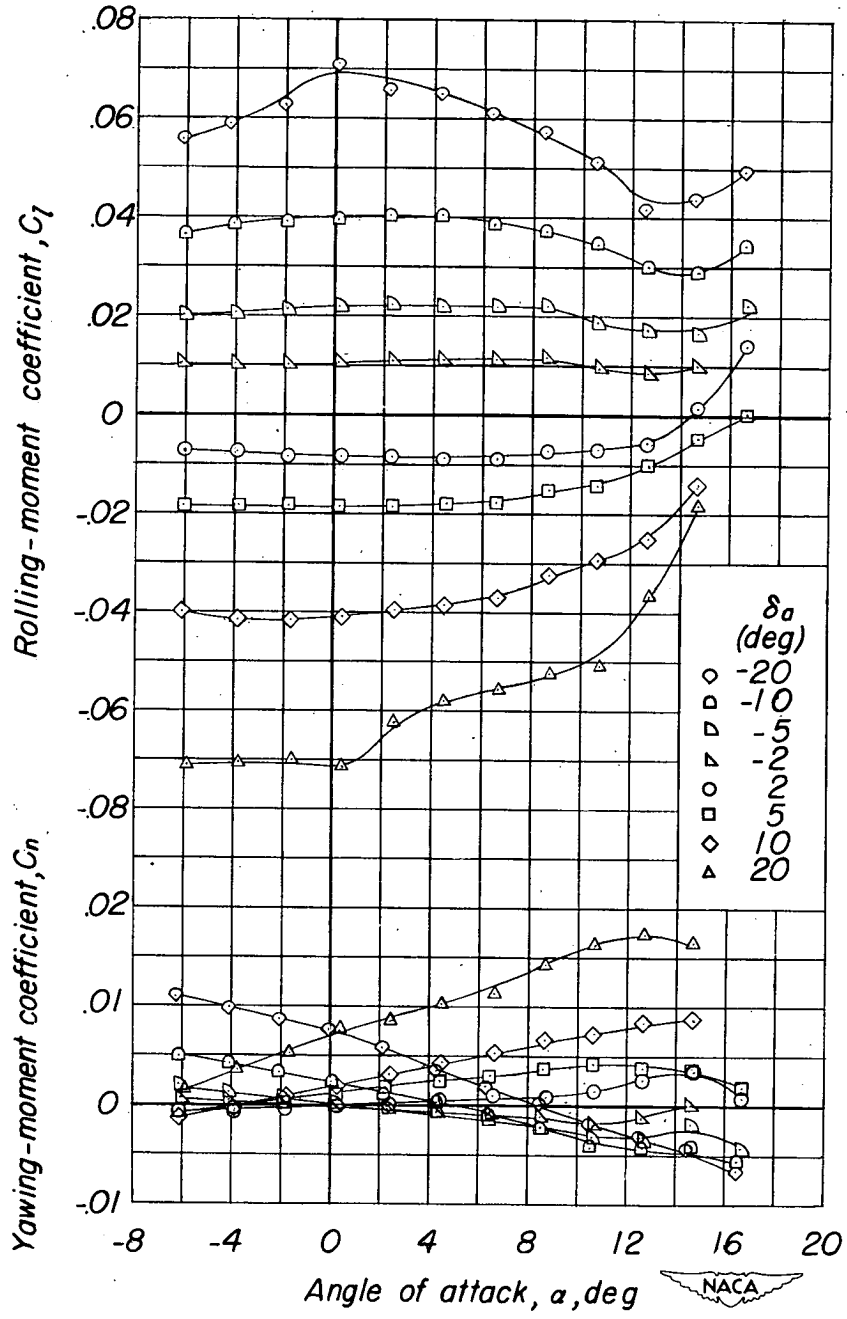

Figure 25.- Variation of the lateral control characteristics of the A = 6.13 wing with angle of attack. Outboard ailerons; $\frac{b_a}{b/2} = 0.746$.

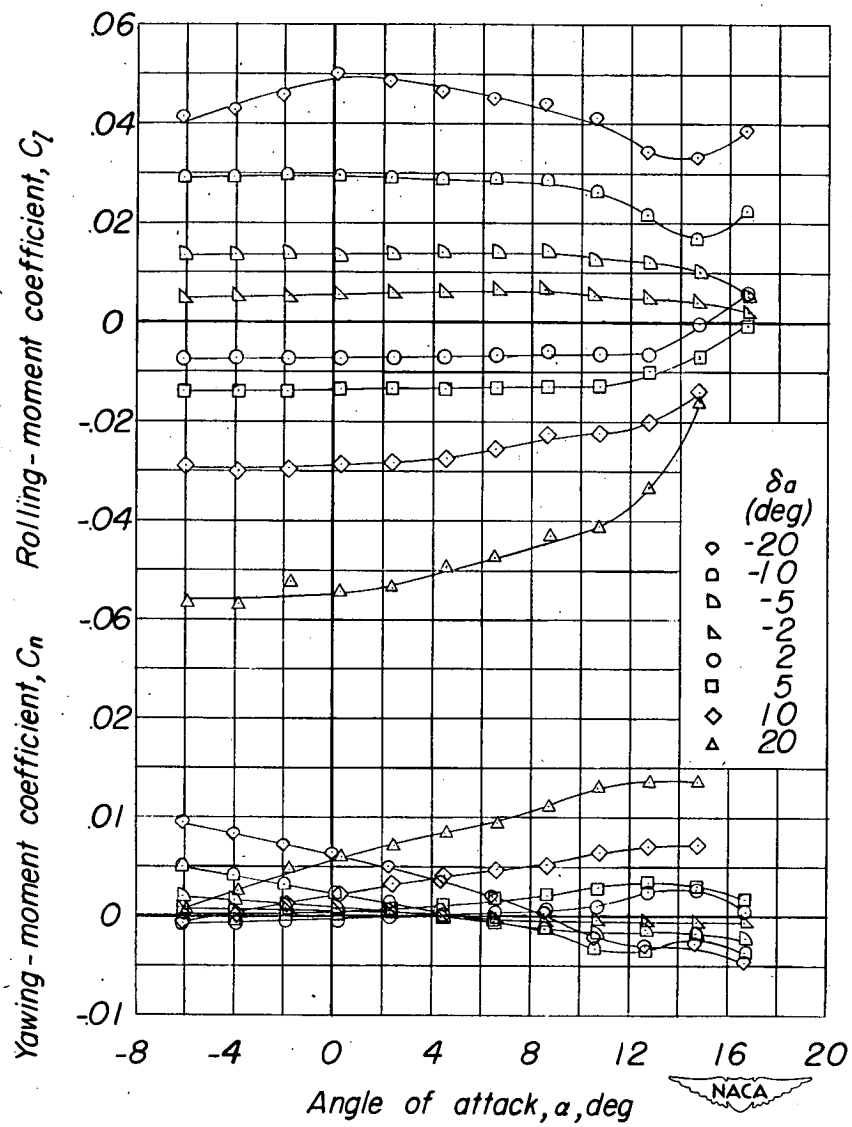

Figure 26.- Variation of the lateral control characteristics of the A = 6.13 wing with angle of attack. Outboard ailerons; $\frac{b_a}{b/2} = 0.500$.

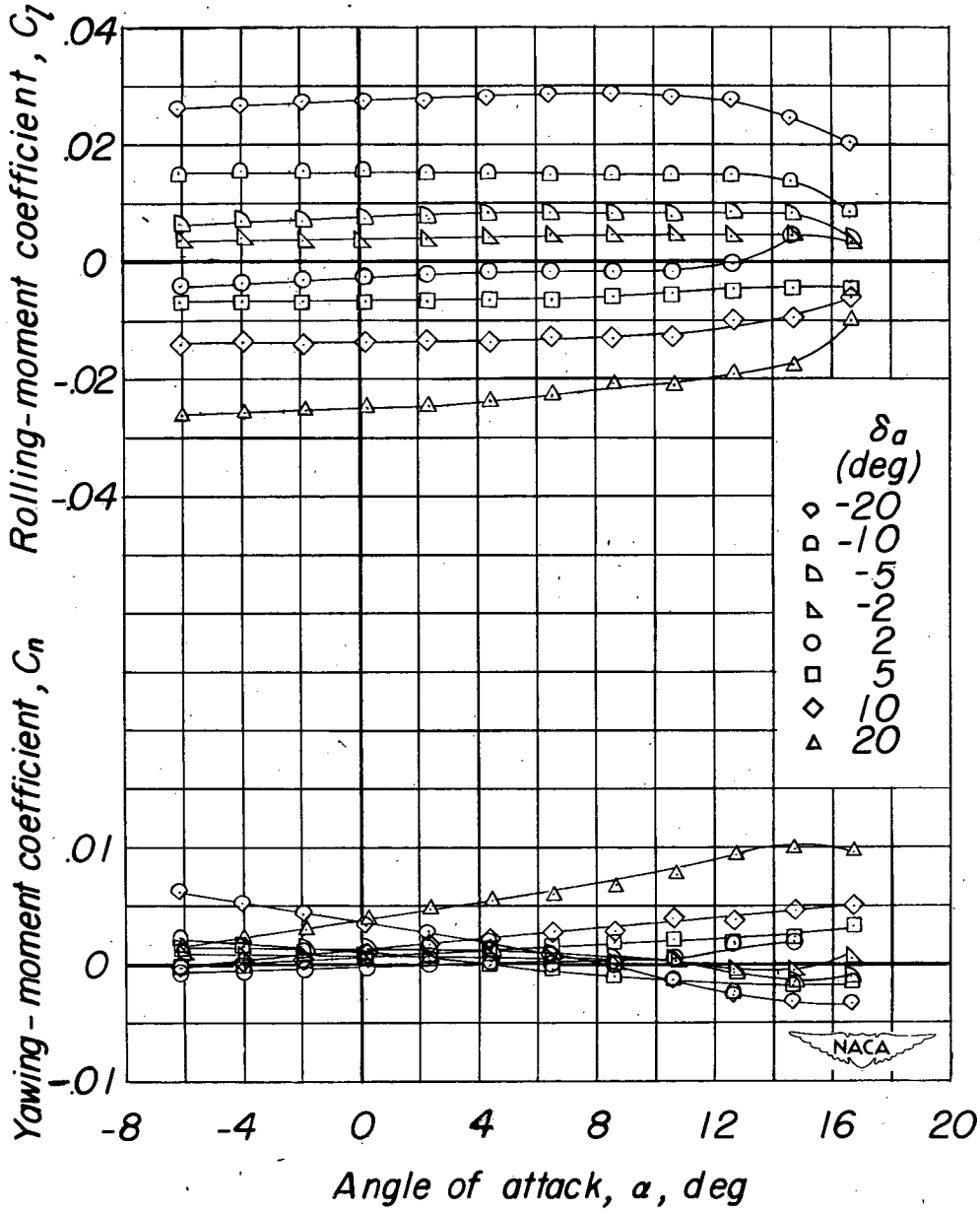

Figure 27.- Variation of the lateral control characteristics of the A = 6.13 wing with angle of attack. Outboard ailerons; $\frac{b_a}{b/2} = 0.254$.

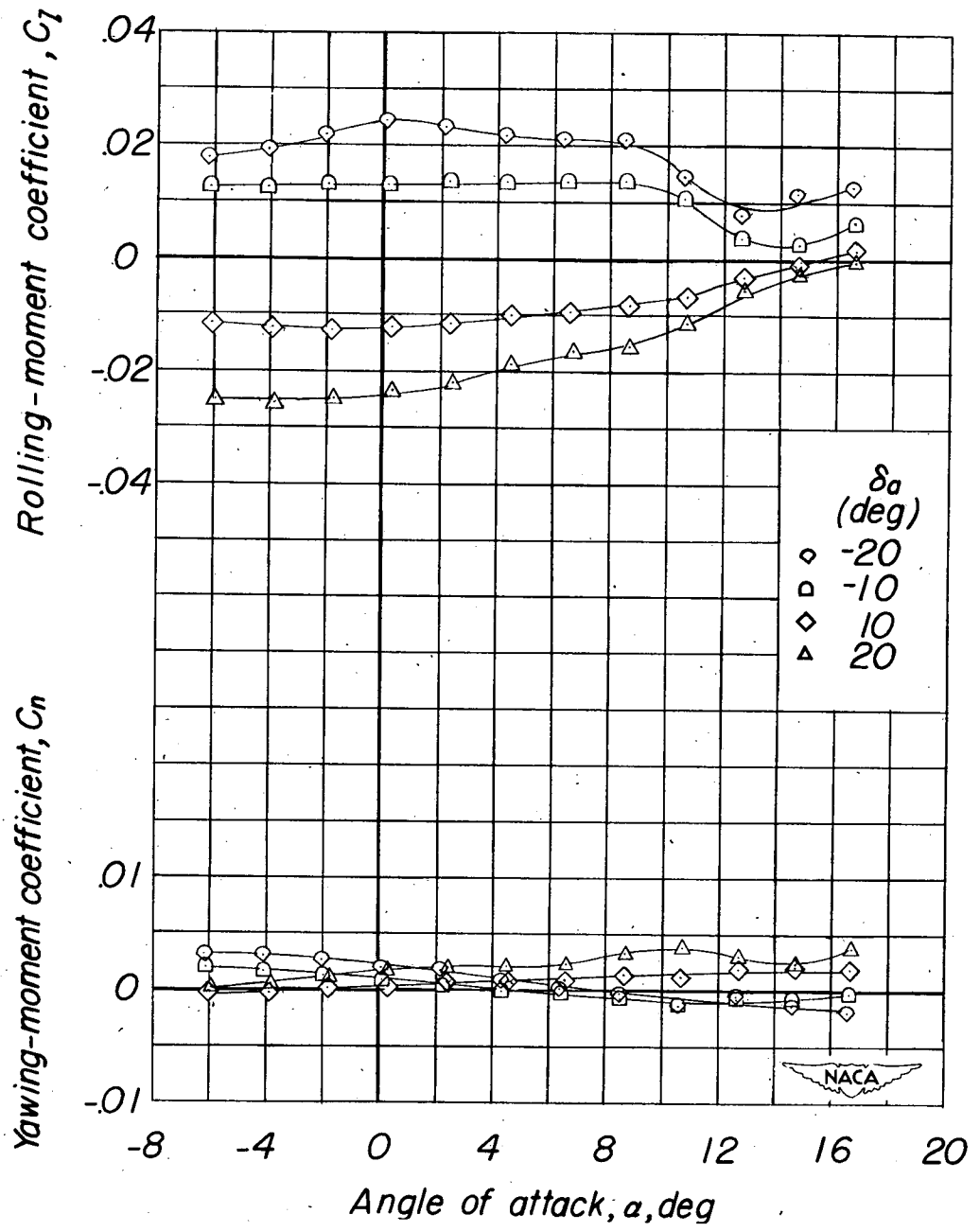

Figure 28.- Variation of the lateral control characteristics of the A = 6.13 wing with angle of attack. Inboard ailerons; $\frac{b_a}{b/2} = 0.425$.

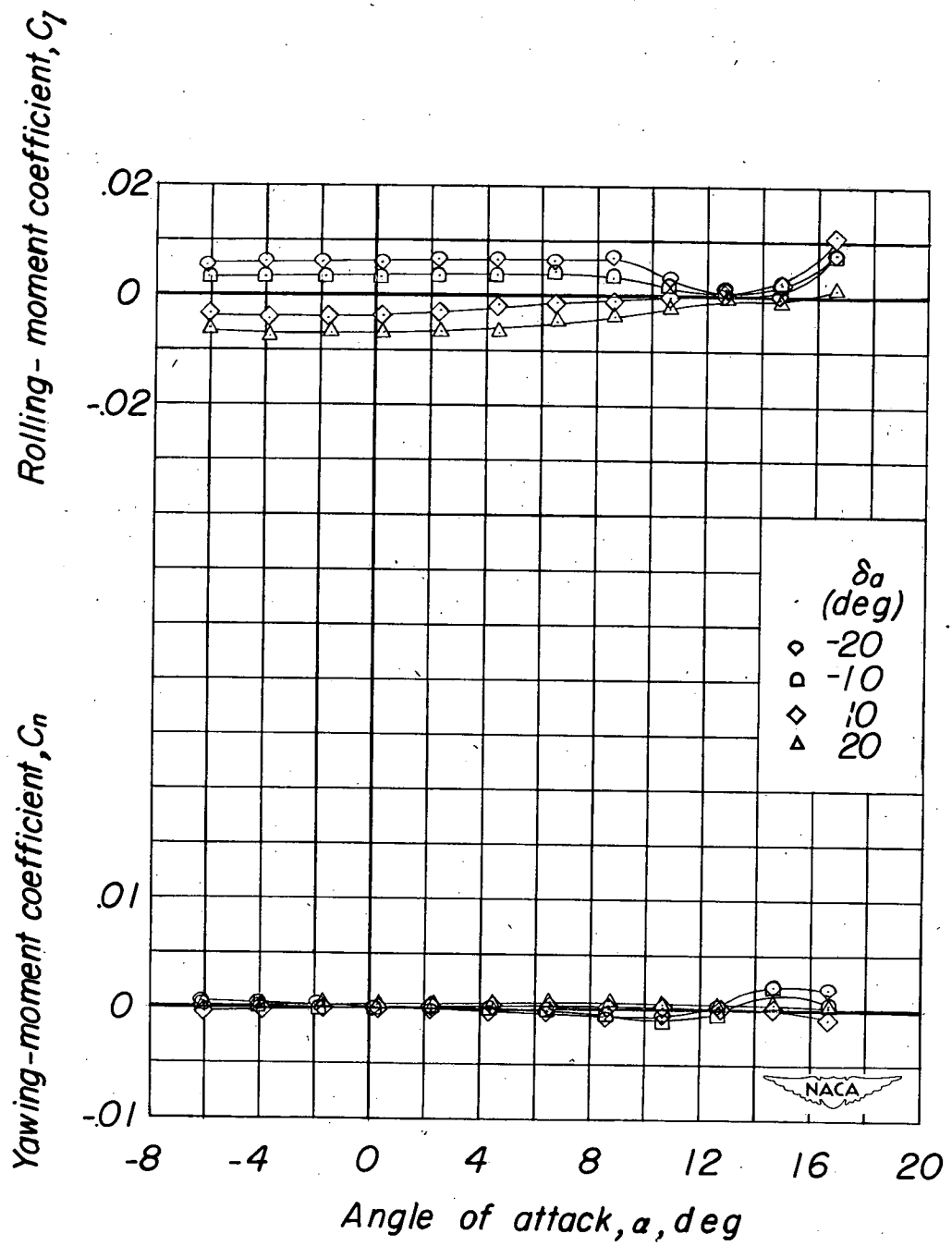

Figure 29.- Variation of the lateral control characteristics of the A = 6.13 wing with angle of attack. Inboard ailerons; $\frac{b_a}{b/2} = 0.179$.

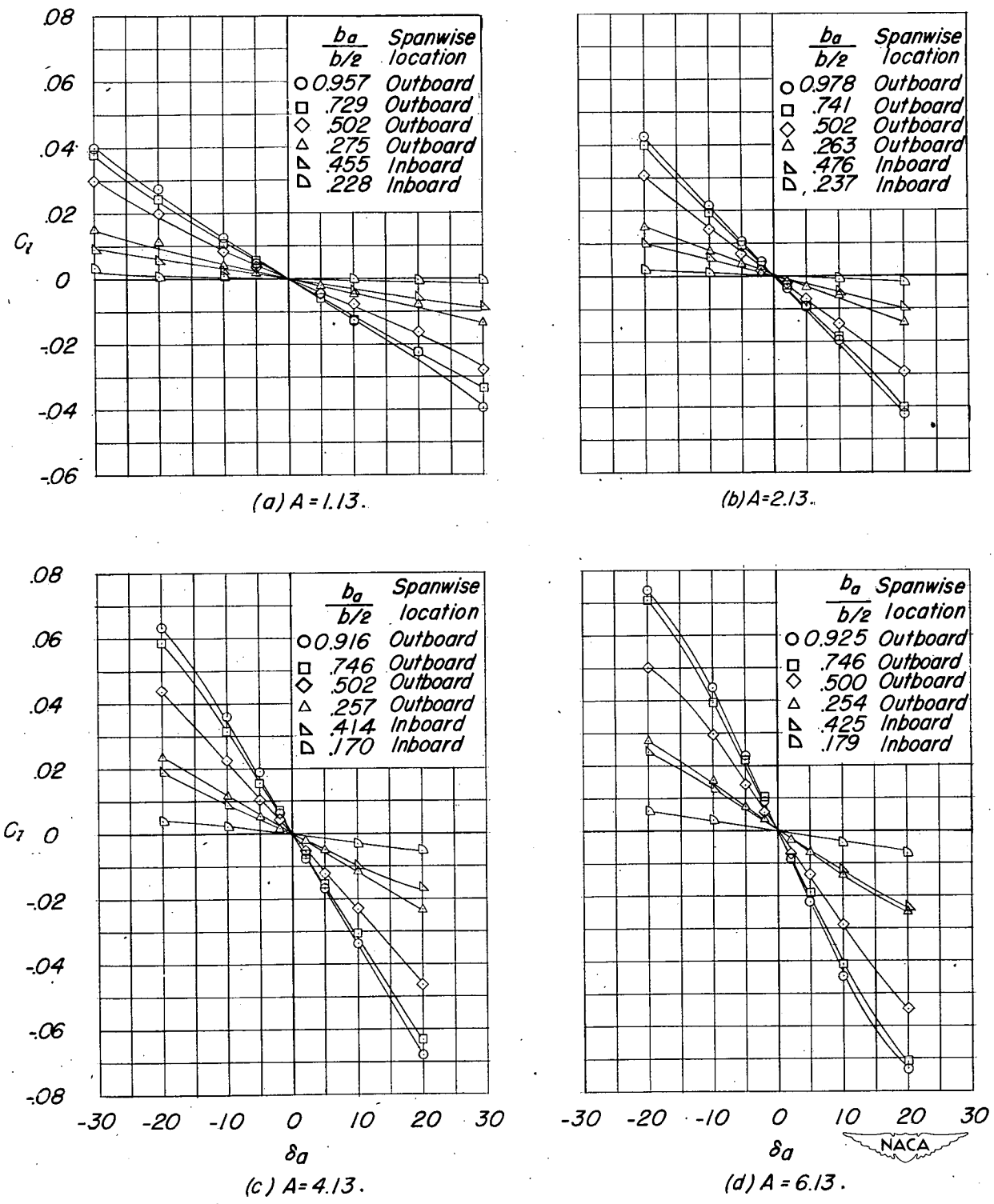

Figure 30.- Variation of rolling-moment coefficient with aileron deflection for various aileron spans. $\alpha \approx 0^\circ$.

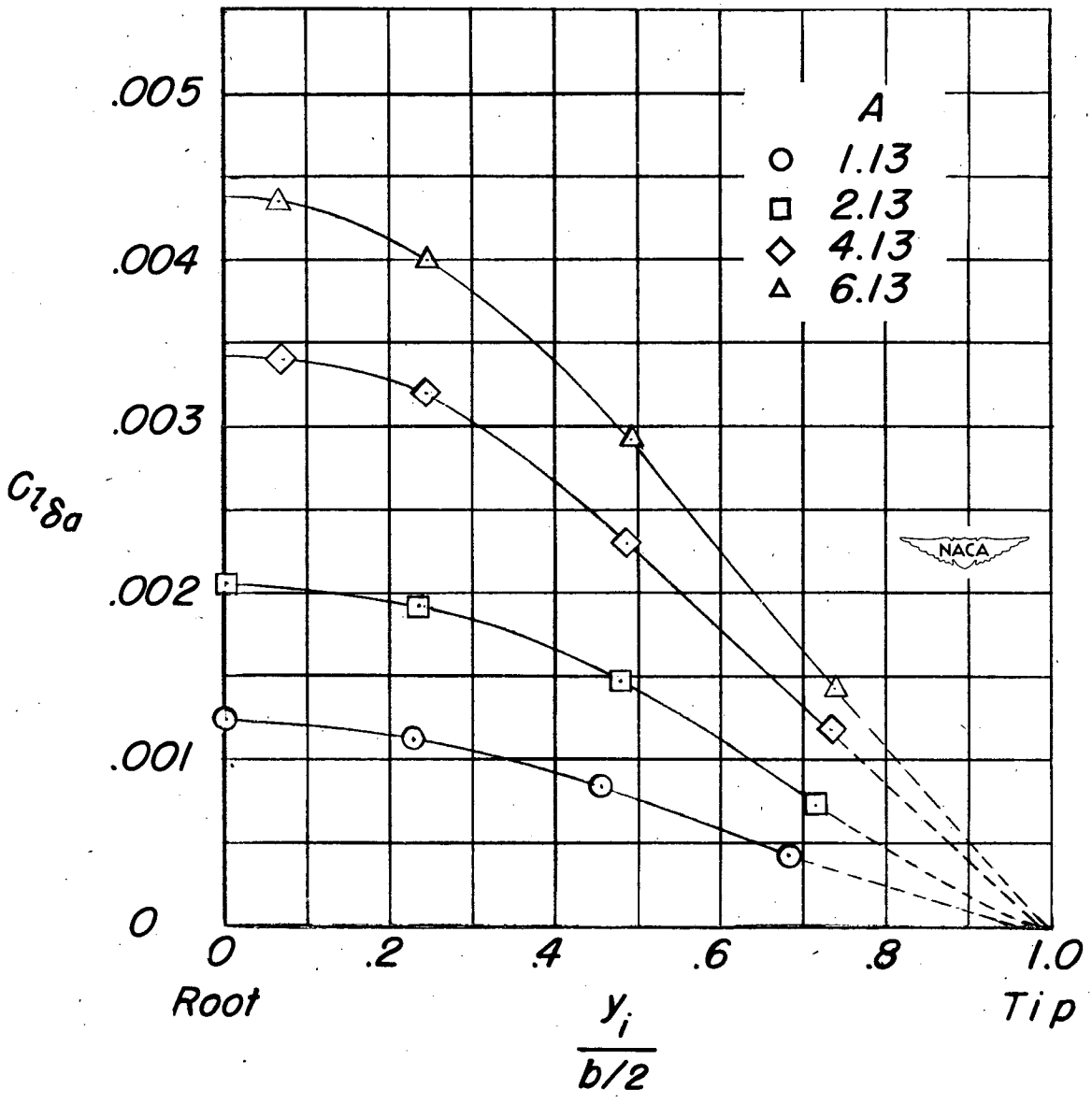

Figure 31.- Aileron effectiveness parameter $C_{l_{\delta_a}}$. $\alpha \approx 0^\circ$; outboard ailerons. The symbols do not represent test points but are used for convenience in cross-plotting the data.

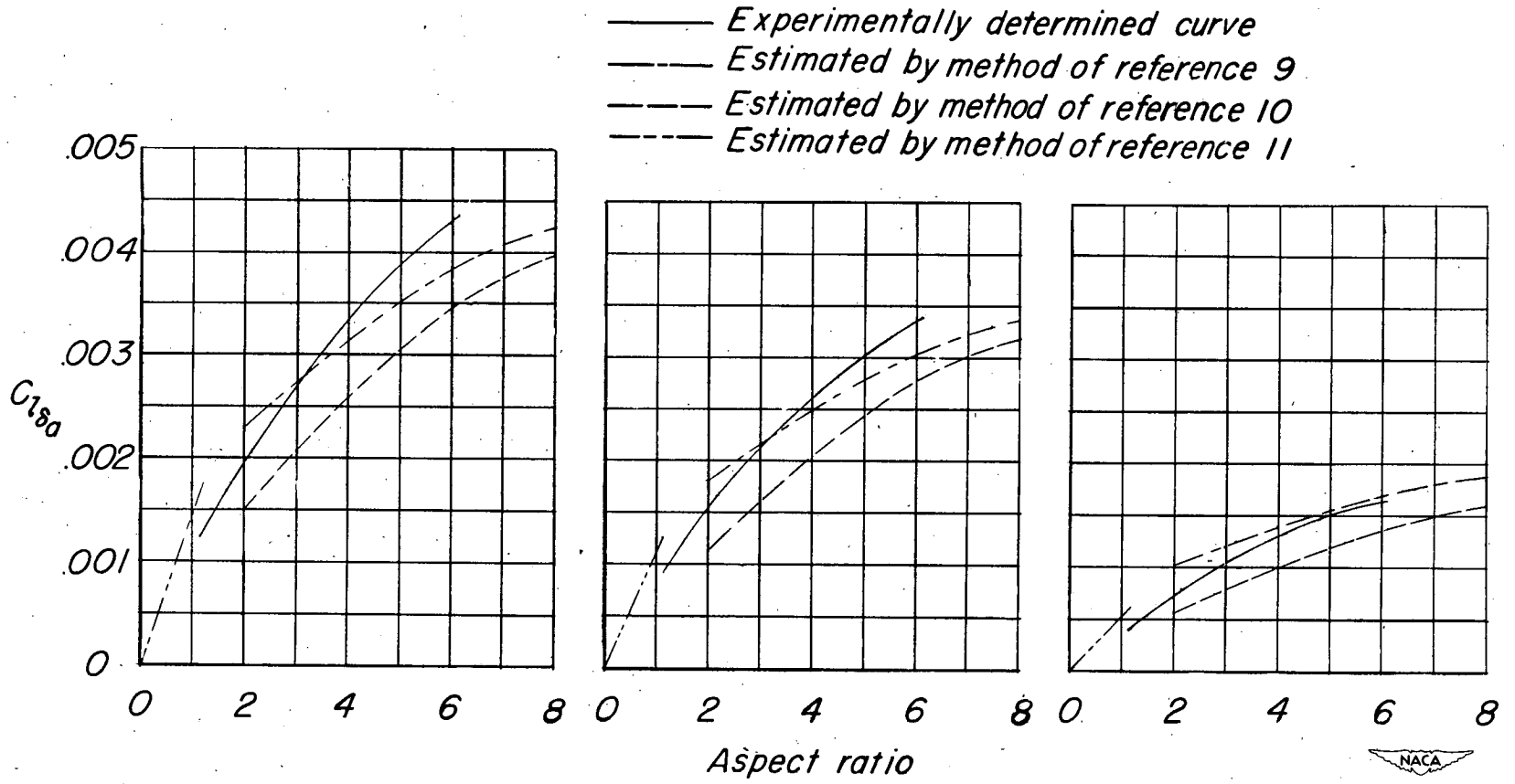

(a) $\frac{b_a}{b/2} = 1.00.$ (b) $\frac{b_a}{b/2} = 0.60.$ (c) $\frac{b_a}{b/2} = 0.30.$

Figure 32.- Variation of aileron effectiveness $C_{l_{\delta_a}}$ with aspect ratio for various spans of outboard ailerons.

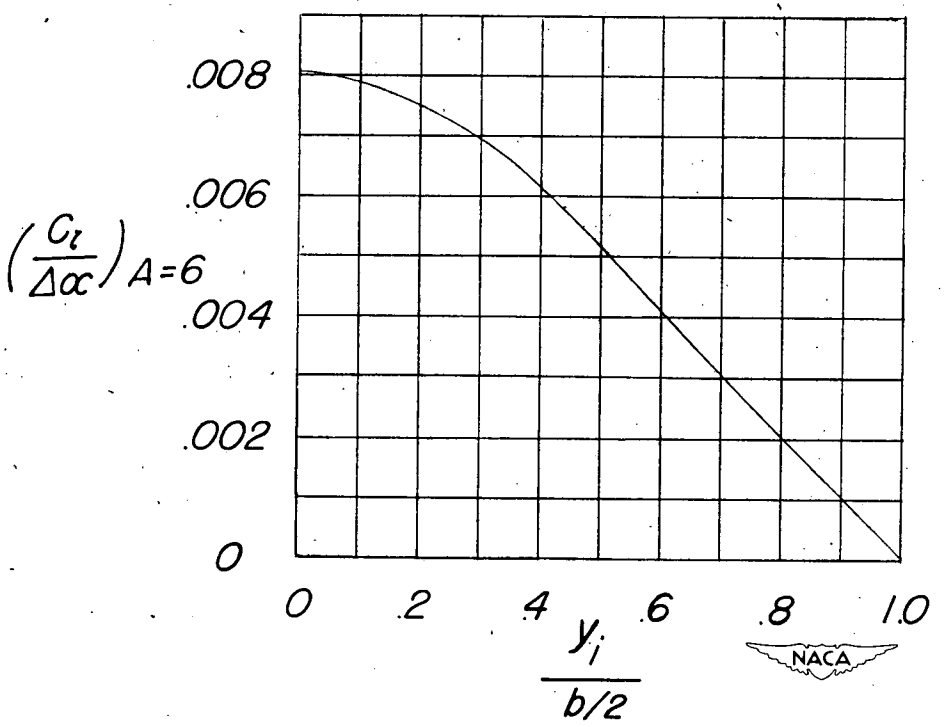

Figure 33.- Variation of values of $\left(\frac{C_l}{\Delta\alpha}\right)_{A=6}$ with aileron span. $C_{l_{\delta_a}} = \left(\frac{C_l}{\Delta\alpha}\right)_{A=6} \alpha_\delta K$.

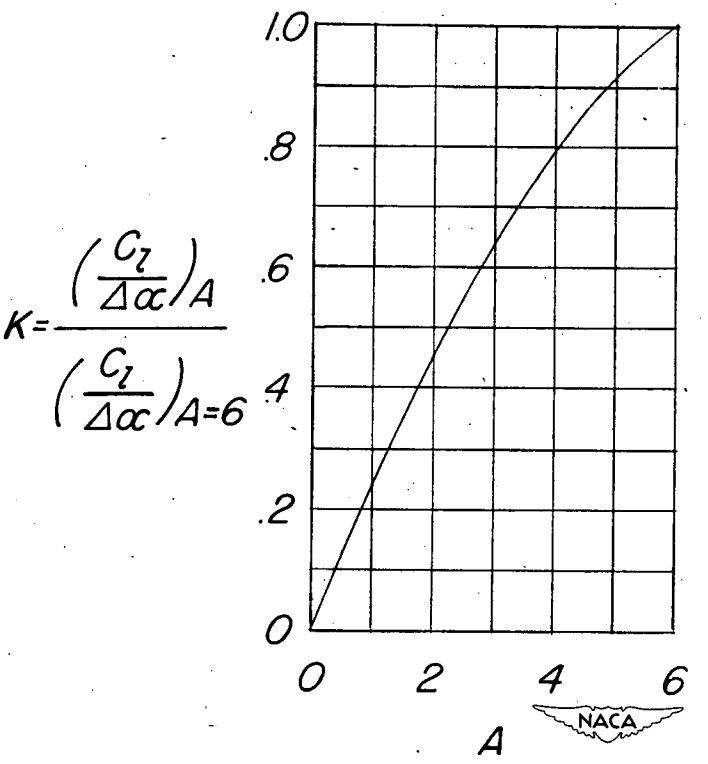

Figure 34.- Factor K for computing $C_{l_{\delta_a}}$.

NACA-Langley - 5-4-51 - 1000

Abstract

A series of untapered, unswept, complete wings of aspect ratios 1.13, 2.13, 4.13, and 6.13 was investigated at a Mach number of 0.26 to determine the effect of aspect ratio on the lateral control characteristics of the wings equipped with 0.25-chord sealed ailerons of various spans and of various spanwise locations. Design charts are presented for computing aileron effectiveness on low-aspect-ratio, untapered, unswept wings. Experimental values of control effectiveness are compared with values estimated by theoretical methods.

Abstract

A series of untapered, unswept, complete wings of aspect ratios 1.13, 2.13, 4.13, and 6.13 was investigated at a Mach number of 0.26 to determine the effect of aspect ratio on the lateral control characteristics of the wings equipped with 0.25-chord sealed ailerons of various spans and of various spanwise locations. Design charts are presented for computing aileron effectiveness on low-aspect-ratio, untapered, unswept wings. Experimental values of control effectiveness are compared with values estimated by theoretical methods.

Abstract

A series of untapered, unswept, complete wings of aspect ratios 1.13, 2.13, 4.13, and 6.13 was investigated at a Mach number of 0.26 to determine the effect of aspect ratio on the lateral control characteristics of the wings equipped with 0.25-chord sealed ailerons of various spans and of various spanwise locations. Design charts are presented for computing aileron effectiveness on low-aspect-ratio, untapered, unswept wings. Experimental values of control effectiveness are compared with values estimated by theoretical methods.

Abstract

A series of untapered, unswept, complete wings of aspect ratios 1.13, 2.13, 4.13, and 6.13 was investigated at a Mach number of 0.26 to determine the effect of aspect ratio on the lateral control characteristics of the wings equipped with 0.25-chord sealed ailerons of various spans and of various spanwise locations. Design charts are presented for computing aileron effectiveness on low-aspect-ratio, untapered, unswept wings. Experimental values of control effectiveness are compared with values estimated by theoretical methods.

Wings, Complete - Aspect Ratio 1.2.2.2.2

NACA

Effect of Aspect Ratio on the Low-Speed Lateral Control Characteristics of Unswept Untapered Low-Aspect-Ratio Wings.

By Rodger L. Naeseth and William M. O'Hare

NACA TN 2348

May 1951

(Abstract on Reverse Side)

Controls, Flap-Type - Complete Wings 1.2.2.4.1

NACA

Effect of Aspect Ratio on the Low-Speed Lateral Control Characteristics of Unswept Untapered Low-Aspect-Ratio Wings.

By Rodger L. Naeseth and William M. O'Hare

NACA TN 2348

May 1951

(Abstract on Reverse Side)

Stability, Longitudinal - Static 1.8.1.1.1

NACA

Effect of Aspect Ratio on the Low-Speed Lateral Control Characteristics of Unswept Untapered Low-Aspect-Ratio Wings.

By Rodger L. Naeseth and William M. O'Hare

NACA TN 2348

May 1951

(Abstract on Reverse Side)

Stability, Lateral - Static 1.8.1.1.2

NACA

Effect of Aspect Ratio on the Low-Speed Lateral Control Characteristics of Unswept Untapered Low-Aspect-Ratio Wings.

By Rodger L. Naeseth and William M. O'Hare

NACA TN 2348

May 1951

(Abstract on Reverse Side)